Pollen Clumping and Release Mechanisms in Wind Pollinated Plants

David Timerman

A Thesis

In

The Department

Of

Biology

Presented in Partial Fulfillment of the Requirements

for the Degree of Master of Science (Biology) at

Concordia University

Montreal, Quebec, Canada

June 2013

Concordia University

School of Graduate Studies

This is to certify that the thesis prepared

By: David Timerman

Entitled: Pollen Clumping and Release Mechanisms in Wind Pollinated Plants

And submitted in partial fulfillment of the requirements for the degree of

Master of Science (Biology)

Complies with the regulations of the University and meets the accepted standards with respect to originality and quality.

Signed by the final Examining Committee:

Dr. Ian Ferguson	Chair
Dr. Jochen A.G. Jaeger	Examiner
Dr. Selvadurai Dayanandan	Examiner
Dr. James W.A. Grant	Examiner
Dr. David F. Greene	Supervisor
Dr. Josef D. Ackerman	Supervisor

Approved by Dr. Selvadurai Dayanandan, Graduate Program Director

Dr. Joanne Locke, Dean of Faculty

July 17, 2013

Abstract

Pollen Clumping and Release Mechanisms in Wind Pollinated Plants

David Timeman

Wind pollinated (anemophilous) angiosperm lineages have often converged independently on floral traits; the syndrome of traits presumably reflecting adaptation to more efficient pollen transport by wind and capture by receptive surfaces. One often-cited trait differentiating anemophiles from zoophiles is the cohesion of pollen grains into clumps, with greater clumping expected among the latter. Further, the mechanism by which grains are released remains underexplored. This thesis examines (1) whether pollen clumping can be used diagnostically to determine the vector, and (2) the hypothesis that resonance vibration of stamens in wind gusts is a mechanism of pollen release. Pollen clumping was studied intraspecifically in the wind pollinated *Plantago lanceolata* and interspecifically across 23 anemophilous and zoophilous species. Mean clump size was found to be well-distinguished species by vector, and the lognormal distribution was a reasonable characterization of clump size for the majority of the species examined. The stamens of *P. lanceolata* were manipulated in the laboratory and observed in the field to characterize their dynamic response to vibration. Stamens had elastic properties corresponding to modeling as underdamped cantilever beams and to theoretical ranges predicted to initiate resonance vibration in wind gusts. Pollen was released in multiple discrete bursts from resonating stamens with successively greater energy requirements. In the field, pollen release was observed from a resonating stamen. Understanding the function of stamen properties is crucial for developing an evolutionary

theory of anemophily and modeling the wind pollination process. This study demonstrates that anemophilous stamens have distinct, quantifiable physical properties differentiating from stamens evolved for other mating systems.

Acknowledgements

Foremost, I thank my supervisors Dr. David F. Greene and Dr. Josef D. Ackerman not only for guiding and supporting this project from start to finish but for believing in my ability to undertake a completely new research program. I also thank Dr. Javier Urzay for introducing me to the concepts of fluid-structure interactions and for his many valuable insights and suggestions.

I am grateful to Sonia Ruiz of the Department of Biology who ensured that I always had adequate space in the growth chambers, greenhouse and in various laboratories. Dan Juras of the Department of Mechanical Engineering had a pivotal role in developing some of the early methodology. Lots of customized technical equipment was built by Richard Allix at Concordia's Science Technical Center. His ingenuity is appreciated.

I conducted field work at the Pro Mata field station in Rio Grande do Sul, Brazil during the 2010 International Pollination Biology course. Thank you to Dr. Peter G. Kevan and the organizers for their logistical support, advice and technical assistance. Field observations were also made at Circle R ranch in London, Ontario. Thank you to the Russell family for their support.

Illustrations in figures 2.1, 2.2, 3.1 and 3.3 were drawn by Sarah Tracy. I am grateful to her and to my lab assistants Amie-Joy Phipps and Geoffrey Frissore. Thank you to my friends and family for of their support and understanding throughout. Thank you to my parents: Sharyn and Gabriel Timerman; siblings: Stephanie and Ellis; cat: Space Tracy; friends: Kirstin Munro, Gail MacInnis, Darsha Hewitt, Kristina Millett, and Alix Rive. I am also very thankful to Scott Monk for generously sharing his many mathematical and technical insights.

Finally, thank you to the NSERC-Canadian Pollination Initiative for their very generous funding and to NSERC and FQRNT for their scholarship support.

Table of Contents

List of Figures

List of Tables

Chapter 1

General Introduction

The spatial range of embryophytes was initially restricted to habitats where sperm cells could move independently toward an ovule within a film of water (Niklas, 1997). The evolution of pollen among the spermatophytes was a major evolutionary transition as it permitted sexual reproduction over longer distances and the colonization of dry environments; i.e., pollen has a waxy or resinous wall protecting the haploid generation from desiccation. In the earliest angiosperms, insects transferred pollen, presumably incidentally, from male to female organs while foraging on flowers, whereas in gymnosperms, this pollination was effected by wind (Proctor et al., 1996). Over time, spermatophytes have developed a variety of generalist and specialist associations with both biotic and abiotic pollination vectors (Waser et al., 1996; Ackerman, 2000; Johnson and Steiner, 2000; Culley et al., 2002; Fenster et al., 2004; Hall and Walter, 2011). More specifically, spermatophytes have evolved contrivances to enhance the probability of viable pollen delivery. These include adaptations for: (1) the release of pollen to the "proper" pollination vectors; (2) the dispersal and survival of in-transit pollen; and (3) its deposition onto female reproductive structures (e.g., Niklas, 1992; Endress, 1996; Edlund et al., 2004; Pacini and Hesse, 2004; Katifori et al., 2010).

Distinct plant lineages often have convergent floral traits called pollination syndromes which are thought to have evolved to increase the efficiency of particular types of pollination vectors (Faegri and Pijl, 1979). This is apparent among the wind-pollinated angiosperms where the anemophilous syndrome evolved from entomophilous

(insect-pollinated) ancestors at least 65 times (Friedman and Barrett, 2009). Floral traits that are commonly associated with anemophily include: the absence of pigmentation, nectar and scent, reduced perianths, feathery styles, smooth pollen grains, high pollen-to-ovule ratio, lessened pollen clumping, and elastic stamens or inflorescences.

As wind pollination is a physical process governed by fluid dynamics, many of these traits may represent solutions to problems of pollen release, dispersal and capture (Ackerman, 2000; Harder and Prusinkiewicz, 2011). However, the evidence favouring this hypothesis is mostly inferential as there have been only a few attempts to experimentally understand the biomechanical significance of any of the typical anemophilous floral traits. Complicating understanding in this field, a growing body of evidence suggests the prevalence of ambophily, a mixed pollination system whereby plants are simultaneously or sequentially pollinated by wind and animals (Culley et al., 2002; Friedman, 2011). Whether ambophily represents a transition state on an evolutionary pathway between pollination syndromes or a long-term opportunistic reproductive strategy is not known, but its occurrence demonstrates the inherent difficulty in assigning functions to floral traits merely on the basis of pollination syndromes.

Recent interest in the mechanistic modeling of aerial pollen dispersal for the forecasting of allergenic concentrations, controls on inter-population gene flow and the prediction of seed set has led to a closer examination of wind pollination processes (Kuparinen, 2006). However, most research focused on the dispersal of pollen while ignoring its release and capture (but see Niklas, 1985). A mechanistic understanding of these processes would permit the inclusion of additional ecological and environmental aspects to dispersal models, improving their accuracy. Furthermore, it would foster

discussion of the underlying selective forces that have produced anemophilous characters, as well as providing a quantitative basis for assessing ambophily.

The investigation of floral traits in pollen release by wind requires an investigation of stamen properties since they are the primary platform from which pollen is presented to pollination vectors (D'Arcy, 1996). Although flowers vary in the openness of their corollas, the stamens of species in most families are exposed to some degree to wind and therefore should have stamen properties which reflect their pollination mode. However, without a biomechanical context for evaluating these properties, their influence on pollen release remains speculative.

In particular, there ought to have been particularly strong selection for characters that promote the release of pollen in obligately anemophilous plants, overcoming the difficulties posed by the aerodynamic boundary layer around a newly dehisced anther (Niklas, 1985). By contrast, the flowers of obligate zoophilous plants should limit pollen release by wind since these grains would be unavailable for biotic pollination. As truly ambophilous plants need to both conserve pollen for floral visitations and release pollen in wind gusts, they should have intermediate traits for controlling pollen release and retention.

Complicating this simple speculative picture of differential selection for abscission traits, is the ambiguous effect of pollen clumping on release and dispersal by wind. The clumping of pollen, for example, has long been associated with zoophilous plants since it is thought to improve siring success and prevent losses to wind (Pacini and Franchi, 1996; Harder and Johnson, 2008). Contradicting this view is a recent study of the anemophilous *Ambrosia artemissifolia* that finds high clumping during release

(Martin et al., 2009). If aeroelastic vibrations of stamens cause inertial pollen release, a clump of pollen would have a greater probability of release than a single grain owing to the larger inertia of the former, provided that the source of cohesion has no more than a linear effect on the adhesion of pollen to the anther (c.f., Urzay et al., 2009). On the other hand, clumping reduces pollen dispersal (by increasing the terminal velocity: Stokes' Law) and thus gene flow (Jackson and Lyford, 1999), and this has been the main argument for why anemophiles tend to show less clumping than zoophiles. It is possible that some anemophiles possess an elegant solution to this problem: both *A. artemissifolia* and the ambophilous *Plantago lanceolata* have clumped pollen that is rapidly disaggregated after release (Tonsor, 1985; Martin et al., 2009). One wonders how common this solution to a biomechanical constraint is among anemophiles and ambophiles.

The question of how clumping affects the probability of release leads to the underlying question: what is the force that effects the release of pollen? That stamens of anemophilous plants are often exserted and oscillate in wind gusts suggests that there is a vibratory release mechanism for wind pollination (Niklas, 1992; Urzay et al., 2009; Harder and Prusinkiewicz, 2011). If so, it should be possible to identify mechanical properties of stamens that determine the operating limits of aerodynamic pollen release. This understanding of physical limits could then be compared across species and pollination syndromes to improve our understanding of the evolution of flowers as structures strongly bounded by physical processes.

No one has yet attempted to verify that the release of pollen in the great bulk of anemophiles is due to vibration, or that clumping might promote the release of pollen by

wind. Other methods of inertial pollen release occur such as the catapulting mechanism of *Morus alba* (anemophilous) and *Cornus canadensis* (ambophilous) and the explosive release mechanism of *Ricinus communis* (anemophilous) (Bianchini and Pacini, 1996; Taylor et al., 2006; Whitaker et al., 2007). A vibrational dispensing mechanism has also been found in a subclass of entomophilous plants termed buzz-pollinated, whereby species of Apidae agitate stamens of Primulaceae, Solanaceae, Ericaceae, Actinidiaceae among others (Buchman and Hurley, 1978; Harder and Barclay, 1994; King and Ferguson, 1994; King and Buchmann, 1996).

Research Objectives

The main objective of this thesis is to examine the role of mechanical vibrations in aerodynamic pollen release in order to stimulate discussion on the selection of stamen characters for the release or retention of pollen as well as to offer empirical insight to dispersal modellers. I conducted a series of experiments to to determine whether or not vibratory pollen shedding is a likely release mechanism for typical anemophilous stamens. As a secondary objective, I also quantified pollen clumping across a number of species in order to determine if there is an explicit relationship with pollination vectors that would consequently satisfy some physical requirements for pollination.

In chapter 2, I begin with a literature review on stamen biology and pollen release. Following are two self-contained research chapters, one of which has already been submitted for publication. Chapter 3 characterizes the dynamic response of anemophilous stamens to mechanical agitations. I hypothesized that excitations within the mechanical energy-containing frequency range of wind gusts would stimulate pollen release. I

examined this hypothesis intraspecifically in *Plantago lanceolata* L. (Plantaginaeceae), an ambophilous species exhibiting strong anemophilous features. While I only studied one species, my ultimate goal was to develop the experimental foundation for a future interspecific comparison. This research may also inform future analytical models of pollen release. In chapter 4, the clumping of *P. lanceolata* pollen was quantified and compared to those of 31 anemophilous and zoophilous species. I introduce a standardized procedure for generating pollen clump size distributions via the random disaggregation of pollen in order to test the hypothesis that the intensity of clumping is dependent on the pollination vector

Chapter 2

Literature Review

Introduction

At least 10% of angiosperms are pollinated by wind and their pollen grains represent some of the most abundant biological particles in the atmosphere (Ackerman, 2000; Linskens and Cresti, 2000; Friedman and Barrett, 2009). Predicting the dynamics of aerodynamic pollen transport has been of considerable interest because atmospheric pollen is important to a number of sectors including public health and in scientific disciplines such as paleobotany, climatology and plant ecology. In public health, for example, inhalation of pollen grains causes acute respiratory symptoms in approximately 15% of the human population (Linskens and Cresti, 2000). Furthermore, because pollen has a chemically inert outer wall, it is prone to fossilization and therefore, pollen bearing deposits form an important record of past vegetation compositions and past climates (Jackson and Lyford, 1999). Most importantly, pollen grains represent the male haploid stage of the angiosperm lifecycle (i.e., the male gametophyte). Consequently, seed production and population dynamics depend on female pollen receipt.

Most recent work (i.e., > 1960) on atmospheric pollen transport has been based on the empirical correlation of dispersal and meteorological data (Kuparinen, 2006). However, this methodology is sensitive to experimental conditions and environmental variation. Therefore, it is problematic to extrapolate the conclusions across populations or years (Kuparinen, 2006). The contemporary approach to this problem is to employ

mechanistic models that are based on the physical theory of airborne particle dispersion. This process-based methodology is effective as it can easily be adapted to include specific characteristics of the study system, including the release mechanism of the pollen grains from the plant (Kuparinen, 2006). Unfortunately, apart from the spatio-temporal and environmental correlates of pollen concentration or flux in the vicinity of a population (e.g. pollen is mainly released during dry, sunny weather), little is known about pollen release mechanisms (Martin et al., 2010). Although there have been some empirical and theoretical investigations of pollen release, they have never been adequately summarized. Therefore, it is the purpose of this review to delineate the current understanding of aerodynamic pollen release mechanisms from the anther.

Pollen Development, Clumping and Anther Dehiscence

The basic male reproductive structure of an angiosperm is the stamen which usually consists of a filament subjacent to a pollen-bearing anther (Fig. 2.1A,B). Although there is considerable variation among taxa in the number of stamens per flower and their morphologies, stamens generally follow a similar ground plan (D'Arcy, 1996). The filament contains vascular tissue which conducts nutrients and water to the anther and the anther is divided into two bilaterally symmetric, reniform lobes called theca each with distinct tissue layers that surround one or more loculus of pollen (i.e., microsporangia; Fig 2.1C,D).

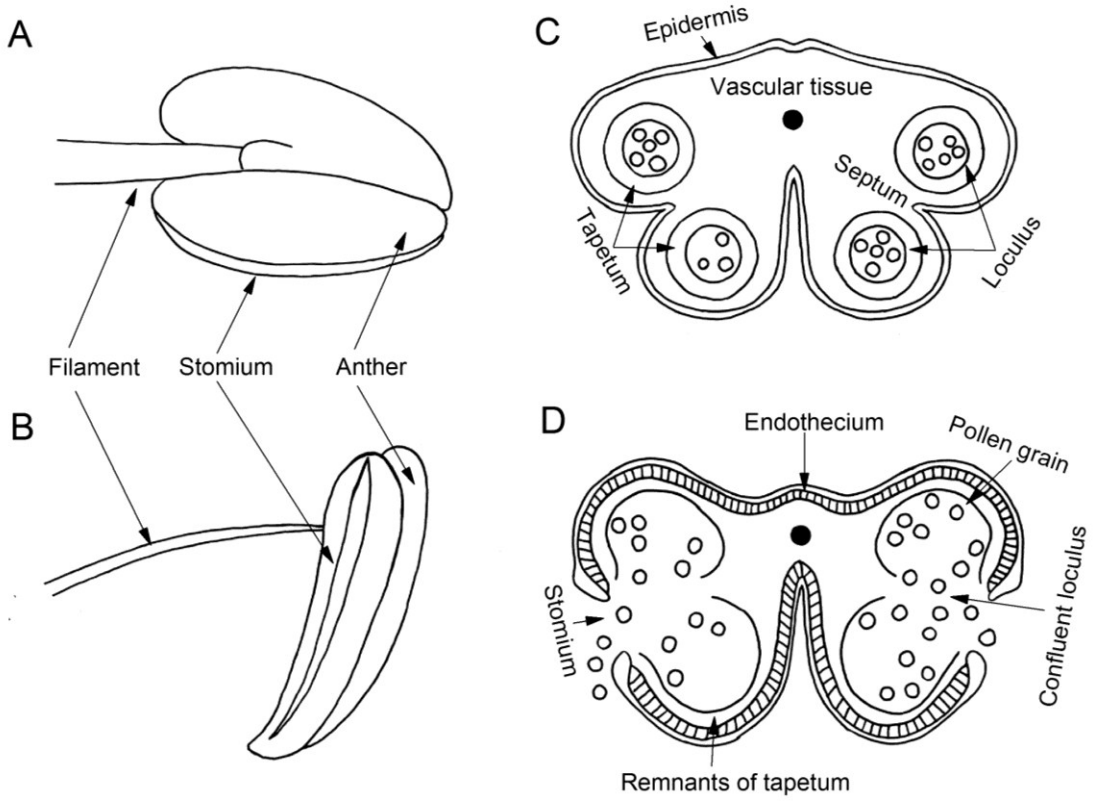

Figure 2.1: Illustrations of typical anther-filament (stamen) configurations and anther cross-sections. Each image depicts a longitudinally dehiscent anther. A) Fixed anther. B) Versatile anther. C) Cross-section of undehisced, fully developed anther. D) Cross-section of dehisced anther. Adapted from D'Arcy (1996).

Many species have pollen grains that are coated with viscous adhesives (pollen glues) causing them to clump to one another or adhere to the interior anther surface and therefore resist pollen release (Pacini and Hesse, 2005). In some zoophilous (animal pollinated) species, the adhesion is so strong that pollen remains on an open anther for weeks. Pollen glues are less common in anemophilous (wind pollinated) plants but are found in cosmopolitan genera such as *Ambrosia* (Asteraceae) and *Plantago* (Plantaginaceae). Pollen glues are derived from layers of tapetal cells that line the inner walls of the loculi. These tissues supply nutrition from the sporophyte that are used in pollen grain development such as sporopollenin, the main structural component of the pollen exine, and callase, an enzyme which separates tetrads of microspores after

microgametogenesis. Once exines are fully formed, the tapetal cells degenerate, spilling their contents onto the surface of the pollen grains (Pacini, 2000). This exudate is an oily, sticky, lipid-rich substance called pollenkitt. In Poaceae and Urticaceae, pollenkitt is mostly absorbed by the individual pollen grains, and thus pollen clumping is limited. Some species produce functional analogs of pollenkitt that differ in ontogeny and composition. These are found in a limited number of families not usually associated with wind pollination such as Brassicaceae (e.g., tryphine) and Orchidaceae (e.g., elastoviscin; Pacini and Hesse, 2004).

There are other mechanisms of pollen clumping that are the result of developmental processes in angiosperms, again not usually found in anemophilous groups, but there are exceptions (Harder and Johnson, 2008). For example, pollen grains are permanently bound into dyads and tetrads if callase fails to dissociate microspores during microgametogenesis. Tetrads are found in at least two anemophilous families, Juncaceae and Cyperaceae (Ali, 1988). These aggregates, as well as individual pollen grains, may also be bound together and to the anther wall by viscin threads, sporopollenin fibers which form during exine development. However, this form of clumping is exceedingly rare, if not completely absent from anemophilous groups. A full review of pollen clumping mechanisms is given by Harder and Johnson (2008).

Orbicules of sporopollenin also form during tapetal degeneration and are found with without pollenkitt on the surface of pollen grains. In anemophilous groups such as Fagaceae and Poaceae they line the inner surface of the loculi. Huysman et al. (1998) have speculated about their function, one of which is the facilitation of pollen release. Since they have the same composition and electrostatic charge as exines, they may reduce

pollen adhesion by electrostatically repelling pollen from the anther. However, there has been no serious study of this mechanism.

Pollen is exposed to the atmosphere by anther dehiscence, a dehydration-driven opening of the anther wall. Dehydration occurs either by evaporation through epidermal stomata, reabsorption of moisture through the vascular tissue, or both. The former is linked to environmental parameters leading to a vapour pressure deficit such as temperature, relative humidity, solar radiation and wind speed. The sudden onset of humid conditions temporarily arrests dehiscence; indeed, the process can be reversed by rehydration in such zoophilous species as *Lilium philadelphicum* (Liliaceae) (Endress, 1996). Reversal of dehiscence is not common in anemophilous plants, although it has been observed in some Poales (Keijzer et al., 1996; Taylor et al., 2002). Reabsorption is an innate process that is regulated by the plant (Dahl et al., 2013). It permits dehiscence in moist environments that do not promote a vapour pressure deficit such as within floral buds, at low latitudes and during overnight hours. Both evaporation and reabsorption operate in certain species, with unfavourable evaporative conditions merely delaying anther dehiscence (Pacini, 2000).

In dehiscence, both theca open almost simultaneously by longitudinal splitting of the stomium, an apoptotic layer of epidermal cells in the furrow between contiguous loculi (Fig. 2.1D). In some Poaceae, such as *Maize*, dehiscence is limited to the apex of the anther (Keijzer et al., 1996). Dehiscence involves the timed cell-death of the septum, forming two loculi, and the stomium, reducing the structural integrity of the anther. This expanded volume rarefies the locular moisture, aiding in dehydration. Confluence also

reduces the number of breakage points required for dehiscence (Pacini and Hesse, 2004). The ultimate arbiters of anther dehiscence are dehydration-driven contractions of the epidermis and secondary lignification of the endothecium,which causes unequal shrinkage of the anther cells. This combination results in differential resistance to bending and stretching leading the anther to bend, fold, rupture and open to a lesser or greater degree. The contractions cause bending while the endothecium provides differential resistance to bending and stretching (Keijzer, 1987; Nelson et al., 2012). In *Ricinus communis* (Euphorbiaceae), a conventional endothecium is lacking; instead there is secondary thickening of the epidermis (Bianchini and Pacini, 1996). After opening, pollen typically remains within the anther until it is released to an airflow.

Stamen Diversity

In spite of the basic organization and development of stamens discussed above, there are considerable combinations of shape, size, anther-filament coupling, and dehiscence patterns that depend not only on phylogenetic history but on pollination ecology (e.g., D'Arcy, 1996; Endress, 1996). This is certainly the case in the zoophilous angiosperms, whose stamens are often modified to enhance biotic pollen collection. For example, in buzz pollination, the filaments of species such as *Actinidia deliciosa* (Actinidiaceae) and *Solanum lacianatum* (Solanaceae) are mechanically optimized to isolate vibrations, generated by apiforme pollinators, onto pollen grains with a minimal loss of energy to the rest of the flower (King and Lengoc, 1993). This causes the explosive release of pollen from the anther, much of which deposits on the pollinator. Furthermore, the anthers of buzz-pollinated species are poricidal, preventing the release

of pollen to non-specialist flower visitors. In some other species (e.g. *Hemerocallis* (Xanthorrhoeaceae) and *Gloriosa* (Colchicaceae)), the anther is free to pivot (*versatile*) on the filament, swinging about when touched and brushing pollen onto pollinators (D'Arcy, 1996). While it is thought that this is an adaptation of flowers to flying pollinators such as moths, butterflies and bats that hover and forage on rewards that are beneath or above the anthers (Endress, 1996), there are anemophiles including species in the Plantaginaceae and Poaceae with versatile anthers.

There is less diversity among stamens of anemophilous taxa, particularly in the anther filament-couplings and dehiscence patterns, as anthers are usually versatile (Fig. 2.1B) or fixed (Fig. 2.1A) upon the filament and they open longitudinally (Fig 2.1A, B) or, less commonly, via apical slits (D'Arcy, 1996; Endress, 1996). Apart from phylogenetic constraints, this may reflect a limit on the number of biomechanical solutions for pollen release into airflows. As flowers of anemophilous taxa have convergent forms, regardless of their diverse lineages, it is likely that salient features of anemophilous flowers, including those of stamens, are functional in pollen release (Ackerman, 2000). For example, the perianths of most anemophilous species are reduced or absent, exposing stamens to higher wind speeds and permitting the unobstructed removal of pollen. Similarly, anthers are often projected away from the boundary layer of the main flower on long, exserted filaments; or away from branches on pendulous structures such as catkins or erect structures such as scapes (Niklas, 1985). For example, both traits are found in *Plantago lanceolata*, whose long horizontal stamens are projected from a spike inforescence on an erect, slender scape (Primack, 1978). Likewise, *Acer saccharinum* has male catkins with very long filaments. In all these cases, since the

boundary layer thickness is inversely proportional to at least the square of the free stream velocity (for the limiting case of a laminar boundary layer; Jones and Harrison, 2004), these structures extending the anther well away from much larger drag-producing bodies, reduce the boundary layer thickness around the anther.

Filaments are also often flexible, elastic and vibratory, as are their supporting structures (Niklas, 1985). This is evident in Poaceae where stamens are thin and fragile, moving even at barely perceptible wind speeds. Their inflorescences are projected onto peduncles that are also prone to vibration. In woody taxa of Aceraceae, Thalictrum and Ulmaceae, more energy is required to excite stems than with herbs but their motions are nonetheless expected to excite or amplify stamen vibrations (e.g., de Langre, 2008). Interestingly, genera having both anemophilous and zoophilous species such as *Acer* (Aceraceae) and *Thalictrum* (Ranunculaceae) are dichotomous in filament structure and stamen exposure with zoophilous species having stamens that are much more rigid, sheltered (by the corolla), and elongate.

But anemophilous filaments need not be long. The microsporangiate catkins of families such as Betulaceae, Fagaceae and Salicaceae bear very short and rigid stamens, albeit with greatly reduced corollas. Presumably the vibration that induces pollen release is supplied by the motion of the entire pendulate catkin rather than, as with long-filamented anemophiles, solely the vibration of the stamen.

Empirical Studies of Pollen Release

There have been very few attempts to relate stamen morphology and physiology to pollen release biomechanics, particularly in anemophilous plants. In *Halophytum ameghinoi* (Halophytaceae), for example, versatile anthers hang freely at the ends of rigid exserted filaments. Under windy conditions, the anthers move from side to side like a pendulum whose speed is changing rapidly. Pozner and Cocucci (2006) hypothesize that this motion pushes pollen towards the apical stomium and out of the anther but this has not been substantiated with experiments or observations. Such versatile anther-filament coupling is common in anemophilous plants of families such as Plantaginaceae and Poaceae, but it is unknown whether or not this rotation has a function in anemophily (D'Arcy, 1996).

Pollen usually remains within the dehisced anthers of wind-pollinated plants unless otherwise disturbed. In controlled environmental chambers drawing air at 0.3 L/min (wind speed was not given but was presumably low), for more than an hour, no pollen was released from dehisced anthers of *Lolium perenne* and *Cynodon dactylon* (Poaceae), *Ulmus parvifolia* (Ulmaceae), and *Betula pendula* (Betulaceae) until they were disturbed with a desk fan (Taylor et al., 2002; Taylor et al., 2004; Miguel et al., 2006). Moreover, pollen release was intermittent in a field study of *Ambrosia artemisiifolia* (Martin et al., 2010). In this species, stamens are fused into a ring surrounding a pistil with a clavate cap of fibers called a pistollidium. After dehiscence, clumped pollen is exuded from the anthers and displayed outside of a tubular corolla. As the pistil elongates, pollen is swept out from the anthers by the pistollidium and drag or shear

forces from turbulent airflows intermittently erodes clumps from the mass of pollen. As specimens in this study were staked to the ground, the effects of whole plant and racemes vibration are unknown.

The mechanics of clumped pollen release in *Ambrosia confertiflora* were recently studied in a wind tunnel using particle image velocimetry and high speed holographic cinematography (Sabban et al. 2012). Pollen was released in large clumps with more than 50% having 150 – 2000 grains per clump at a free stream velocity of 1.0 – 2.0 m/s. Mean initial clump size increased with velocity. A high shear (> 100-200 s^{-1}) in the vicinity of the flower was responsible for the initial release event. Following release, small clumps broke from larger clumps, presumably also by shearing. Fracturing of large clumps did not occur at 1.0 m/s but did at higher wind speeds. Smaller clumps had greater release velocities than larger clumps and tended to travel farther than large clumps (> 4000 grains per clumps). The effects of relative humidity were not studied.

The effect of wind-induced swaying on pollen release was studied by Friedman and Harder (2004) in a number of Poales, demonstrating the interplay of inflorescence architecture and plant movement. Pollen removal was measured 5 hours after dehiscence for manipulated and control plants. Treatments included compaction of diffuse panicles of *Bromus inermis* and *Anthoxanthum nitens* and immobilization by tying individuals with diffuse panicles (*B. inermis* and *Festuca campestris*) and compact panicles (*Elymus repens, Leymus innovatus* and *Phleum pretense*) to stakes. Pollen removal was consistently reduced for the compaction treatment and similarly reduced for compact

panicles in the immobilization treatment suggesting an important role of dynamic loading in pollen release.

Pollen release does not always require the application of external forces; rather, intrinsic mechanisms may cause ballistic release into an airstream. For example, *Ricinus communis* has explosive pollen release (Bianchini and Pacini, 1996). This species has anthers with only one theca and a wall consisting of a single epidermal cell layer with no endothecium, which are uncommon features among angiosperms (c.f., D'Arcy, 1996). The epidermis consists of four cell types each with varying amounts of secondary lignification and cuticle thickness. During dehiscence, there is differential dehydration of cells resulting in centrifugal forces causing the anther to open at the stomium and the loculus to rapidly invert. Pollen grains are exposed to the atmosphere but remain attached to the anther with pollenkitt. The sudden reversion of the loculus generates an impulse that rapidly detaches grains from the anther. This process is delayed at high humidity and completely arrested at saturation. Furthermore, the initial dispersal distance in still air is inversely related to relative humidity. This implies that there is more force resisting the mobilization of the pollen at high humidity.

In some species, the stamen develops under increasing elastic tension that, when released, causes the anther to undergo a catapulting motion, inertially releasing pollen. This mechanism was observed as early as the 18th century in the Mediterranean weed, *Parietaria judaica* (Urticaceae) and more recently its histology has been examined (Taylor et al., 2006; Franchi et al., 2007). The flowers are initially small, approximately 1.0-2.0 mm and grow in clusters of six or seven bisexual flowers surrounding a unisexual

female. Female function precedes male functioning by a few days (protogyny) during which the perianth enlarges and the four stamens elongate to approximately 3.5 mm in length. The filaments are incurved, forming an arc towards the floral axis and compressing the anthers against one another. The anthers lack the structural thickening of the endothecium and epidermis that is common among angiosperms. Following anthesis, the anthers dehydrate and shrink, releasing the tension between them. This causes the filaments to snap backwards rapidly, accelerating the pollen grains, rupturing the stomium and permitting their release. Presumably, the lack of lignification of the anther facilitates this form of dehiscence. Pollen release is asynchronous among flowers but occurs simultaneously for anthers within a flower.

The sudden release of stored elastic energy from the stamens of *Morus alba* (Moraceae) results in one of the fastest motions (160 – 237 m/s) observed in all of biology, exceeding the typical surface speeds of Category 5 hurricanes, and catapulting pollen as far as 66 mm or approximately 2900 times the diameter of the pollen grains (Taylor et al., 2006) despite the tremendous drag operating on the grain at this speed. This species is variously monoecious or dioecious with flowers held on pendulate unisexual catkins 2.0 - 3.5 cm long. Within floral buds are four inflexed stamens clasped by tepals that are physically bound to stomia by fine threads. Initially, the filaments swell with water, some of which is presumably absorbed from the drying anthers. The swelling filament pushes the anthers towards the pistillode, a vestige of female function which restrains further motion. Dehydration of the anthers forces the anthers to pull away from the tepal and abut the pistillode. Tension builds in the threads, causing the stomia to rip open. Since dehydration of the anther occurs before anthesis, it is probably under the

control of intrinsic mechanisms. After 10 seconds, the anthers slip from the pistillode allowing the filaments to rapidly straighten, bursting from the bud and catapulting pollen. Finally, the release velocity is partially under the control of relative humidity and flower age (e.g., velocity is inversely proportional to relative humidity).

Theoretical Studies of Pollen Release

Pollen release has been compared to the release of particles from motionless flat substrates and may therefore be conceptually similar to the release of fungal spores from infected leaves (provided that there is no significant leaf flutter) or the erosion of sand and soil (Grace and Collins, 1976; Niklas, 1985; Jackson and Lyford, 1999; Jones and Harrison, 2004). In contrast to the terminology of Niklas (1992) who calls this an active release mechanism, here it is referred to as a wind-induced mechanism to distinguish it from those that are intrinsic (i.e., not relying on external forces) to a species (e.g., explosive pollen release, ballistic release of some fungal species). The passive release of pollen from a flat substrate depends on a balance of forces. Aerodynamic forces such as drag,lift and shear stress (force/area) cause pollen to translate, rotate and physically detach whereas resistive forces hinder such motions.

The threshold wind velocity required to release pollen sized particles (diameter, D = 30 – 90 μm; Niklas, 1985) is found by balancing the moment tending to hold particles to the surface and the opposing moment generated by aerodynamic forces (Niklas, 1985). Urzay et al. (2009) used a similar approach to approximate the steady Stokes drag force acting on a grain at rest on an anther-sized surface at moderate wind speeds. When

compared to very crude estimates of resistive forces, drag was found to be large enough to release pollen.

Likewise, Grace and Collins (1976) used the theory of steady flows to predict the threshold wind speed to release *Lycopodium* spores (D=33 μm) from a flat surface. Although the theoretical threshold at spore height was only 0.018 m/s, in an experiment, wind speeds as high as 5-7 m/s were needed to liberate the first 50% of spores. However, as pointed out by Aylor and Parlange (1975), spores are held within a boundary layer where wind speeds decline rapidly towards the surface. On a leaf surface mean velocity must be 25 m/s to force 5 m/s wind speeds within the boundary layer (Aylor and Parlange, 1975). Since spores and other particles are often released by much weaker winds, this theoretical formulation clearly under-estimates the threshold velocity.

Studying the liberation of *Helminthosporium maydis* spores from the surface of infected host plant leaves, Aylor and Parlange (1975) found that spores were released even when ambient speed was well below the experimentally determined threshold speed (Aylor, 1975). They hypothesized that wind gusts briefly swept aside the boundary layer air allowing gust speed to reach the surface before the boundary layer reformed. Unlike spores, the effect of wind gusts (unsteady flow) on anther boundary layers has not been investigated. However, Urzay et al. (2009) disputed this solution for pollen grains, arguing that the boundary layer should re-establish to at least the pollen grain mean diameter before a steady state is reached.

These models are all limited to the special case where pollen grains or spores are at rest on a motionless, flat plane. Urzay et al. (2009) adopted a more realistic representation based on the observation that wind pollination often occurs in gusty environments and mechanical agitation of stamens or of their supporting structures are common. Their model corresponds to a linear damped oscillator driven by stochastic wind fluctuations. It predicts that pollen grains will be ejected from the anthers of a resonating stamen when the inertial force on pollen grains exceeds the sum of the resistive forces. When parameterized for a species, this approach has the added potential benefit of incorporating within the resistive force term, the effects of the complex curvature and roughened surface of the anther, the shape of the pollen grains, the adhesive strength of pollen glues and any number of species-specific characteristics. Whether or not gusts initiate these aeroelastic vibrations is an open question but it is a useful, general starting point for discussing the biomechanics of pollen release in the absence of intrinsic release mechanisms.

Interestingly, vibratory release of spores and pollen has been found in a number of fungal and zoophilous plant species. For example, the fungi *Cladosporium caryigenum, Erysiphe graminis, Penicillium* sp. and *Pseudomonas destructor* all release spores by wind-induced shaking of their supporting structures (Grace, 1977). The force (F) required to detach spores, however, has only been measured for *Helminthosporium maydis* ($F=1\times10^{-7}$ N) and *E. graminis* ($F=6\text{x}10^{-12}$ N). Similarly, a subset of zoophilous plants, termed buzz pollinated, rely on mechanical agitation of their stamens by apiformes for pollen release. The resistive force for buzz pollinated plants has been measured for *Actinidia deliciosa* ($F=1.63\text{x}10^{-10}$ N) (King and Lengoc, 1993) and *Solanum lacianatum*

($F=2.2x10^{-9}$ N) (King and Buchmann, 1996). The resistive force for vibratory pollen release has also been measured for a non-buzz zoophilous species, *Rhododendron* spp. (Ericaceae) ($F=1.5x10^{-9}$ N) and does not differ greatly from the buzz pollinated species (King and Buchmann, 1995).

Factors Affecting the Resistive Force

Thresholds for pollen release are determined in part by the forces resisting the mobilization of pollen. Therefore, it is important to understand the nature of resistive forces in order to determine the range of environmental conditions favouring removal and, consequently, the rate of pollen release. The presence of even a small amount of moisture within a fine powder, such as pollen, can profoundly alter its dynamic properties. The adhesive and cohesive forces within the anther, however, have not been studied. Nevertheless, given the rich theory available from particle science and technology, it is possible to make some generalizations (Barbosa-Canovas, 2005). This branch of science is concerned with the individual and bulk properties of granular material such as powders and is concerned with a wide range of topics including the formation of aerosols, crystallization processes and slurry filtration (Rhodes, 1998).

The main types of forces that may influence the threshold for release are gravitational, frictional, mechanical interlocking, liquid bridging, electrostatic and van-der-Waals (Barbosa-Canovas, 2005). These forces may occur individually or in combination. Active mechanisms and aerodynamic forces must overcome the weight of pollen (Fig. 2.2A). This is less problematic for active release mechanisms which launch

pollen at accelerations many times higher than gravitational acceleration. Passive release mechanisms may be more affected by gravitational forces because a greater force may be required to mobilize heavier particles, including clumps. This is because the moment (torque) due to aerodynamic forces is counterbalanced by an opposing moment due to the weight of the particle (e.g., Niklas, 1985; Jackson and Lyford, 1999). Conversely, heavier particles may be preferentially released over lighter particles (including clumps) during vibration pollen release due to the greater inertia of the former.

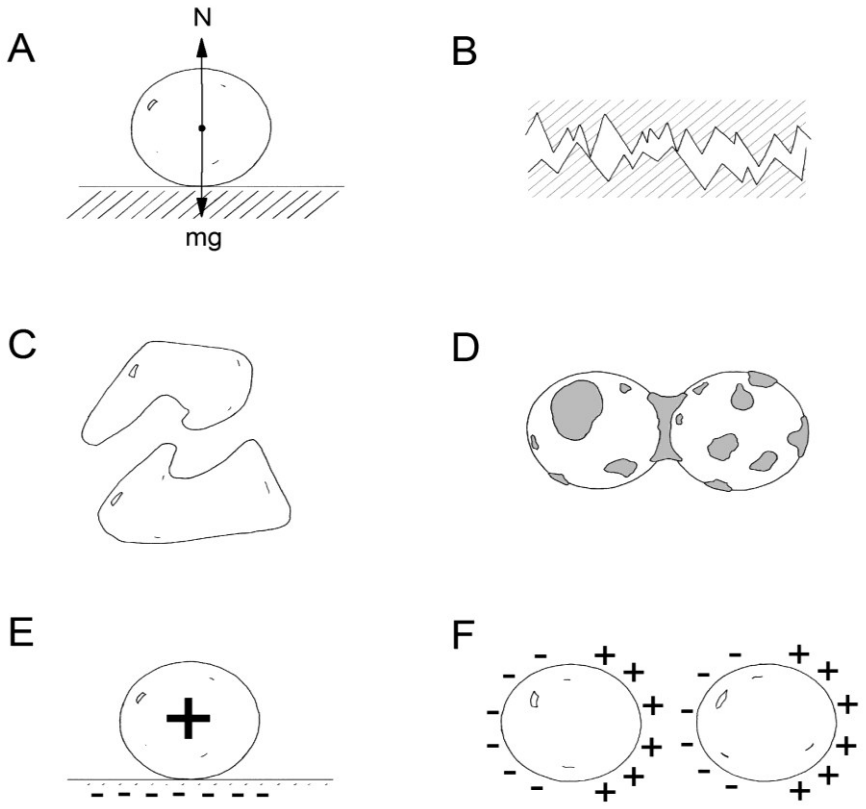

Figure 2.2: Schematic view of factors influencing the resistive forces on pollen grain. Scale is invariant. A) Pollen grain at rest on a surface, depicting the weight (mg) and normal force (N). B) View of two surfaces in contact, showing the microscopic surface roughness between them that leads to frictional force. C) Illustrates how two eccentrically shaped particles can join together, becoming interlocked. The second particle could also be a surface. D) Liquid bridging of two particles. Shaded regions represent a hypothetical viscous compound. E) Electrostatic configuration of a positively charged particle and a negatively charged surface. The surface could also be replaced by a negatively charged particle. F) Depiction of the van-der-Waals force between two particles. One particle could be replaced by a surface. B-D adapted from Clayton (2013). Note that these mechanisms are not mutually exclusive.

By definition, frictional forces inhibit movement between pollen grains or between pollen grains and the anther surface (Barbosa-Canovas, 2005). The strength of the frictional force generally depends on the surface roughness of both surfaces, with smoother surfaces exhibiting less friction (Fig. 2.2B). Compared to zoophilous pollen, anemophilous grains typically have unornamented, smooth exines (Ackerman, 2000) but there is still some surface roughness. In genera such as *Ambrosia*, however, pollen grains are markedly rough (Martin et al., 2009) and should have correspondingly higher coefficients of friction. The weight of pollen is another factor influencing the frictional force which, for a pollen grain on a flat horizontal anther, is linearly proportional to the normal force (e.g., the force that is perpendicular to the surface of contact). Again, relative to zoophilous taxa, anemophilous plants have evolved smaller, light weight pollen grains, which may be an artefact of their higher allocation to pollen number (relative to zoophiles; Cruden, 2000) but may also minimize the resistive forces.

Mechanical interlocking is related to the shape and size of pollen grains, which, as in puzzle pieces, if orientated in a particular way, can cause irregularly shaped pollen grains to lock together or to the roughened surface of the anther (Fig. 2.2C; Barbosa-Canovas, 2005). The potential for this resistive mechanism should depend on the pollen water content and on the distribution of pollen grain diameters. Before dehiscence, pollen either absorbs or expels water (Franchi et al., 2002). Partially hydrated pollen (PHP) grains have a water content of 30% or more and retain a circular shape. PHP pollen is an adaptation of species to quickly germinate after deposition on a stigma (Franchi et al., 2002). The tradeoff, however, is that PHP pollen is metabolically active and is more prone to environmental damage. Pollen grains whose water content is less than 30% are

partially dehydrated (PDP) and speculatively, are most likely to have mechanical interlocking because they lose sphericity and have a range of irregular shapes. This process is mostly under physiological control but pollen may also fold in on itself in response to low relative humidity after dehiscence (Katifori et al., 2010). PDP pollen is more resistant to environmental stress but takes much longer to rehydrate and then germinate on the stigma. Finally, in PDP pollen, a pollen diameter distribution with a large coefficient of variation should result in a greater assortment of shapes and sizes which may promote greater mechanical interlocking.

Liquid bridging via interstitial liquid droplets results in capillary and viscous forces between pollen grains and between pollen grains and the anther wall (Fig. 2.2D; Barbosa-Canovas, 2005). It is the primary means by which pollen clumps and is therefore related to the amount of pollenkitt present (King and Lengoc, 1993; Harder and Johnson, 2008). If water remains after dehiscence or if water vapour is subsequently adsorbed at high relative humidity, an interstitial bridge may form. The formation of bridges by adsorption is related to the surface roughness of the particle, with rougher surfaces requiring higher relative humidity and more time for the bridge to form (Walton, 2008). Provided there is a vapour pressure deficit in the vicinity of the anther, evaporation should reduce adhesion due to liquid bridging over time. This occurs in the buzz pollinated *Actinidia deliciosa* whose pollen grains become less clumped and sticky with time (King and Ferguson, 1994). Interestingly, the force exerted on the fluid bridge of *A. deliciosa* was calculated by King and Lengoc (1993) and found to be 5% higher than the calculated allowable stress (e.g., the force was sufficient to sever the bridge) at the time of vibration-induced release.

Electrostatic or van-der-Waals forces are common sources of adhesion and cohesion in fine particles (Barbosa-Canovas, 2005). Electrostatic forces originate from the transfer of electrons at the interface of bonding materials, thus causing their attraction (Fig. 2.2E). Bowker and Crenshaw (2007) recently showed that the pollen of seven anemophilous species carries charge immediately after pollen release.. Within a species, pollen had a distribution of charges ranging from negative to positive. If pollen has differential charge within anthers, electrostatic forces may be a source of cohesion between pollen grains. However, the presence of moisture may discharge pollen, disrupting the electrostatic attraction (Walton, 2008). As anemophilous plants frequently have dry but clumped pollen (c.f. Hall and Walter, 2011; Timerman et al. Chapter 4), electrostatic forces may be an important component of aerodynamic pollen release. Moreover, as plants frequently carry a negative charge, some pollen may also have an electrostatic attraction to the anther. Finally, van-der-Waals forces arise from instantaneous fluctuations within the atoms that comprise pollen grains (e.g., dipole moments; Fig. 2.2F). This induces an attractive force that declines rapidly with increasing separation between particles. The attractive strength also relies on surface features and size of the particle. As with electrostatic forces, moisture interrupts the van-der-Waals forces.

Conclusion

In this review, several pollen release mechanisms have been identified. These are broadly classified as mechanisms that are intrinsic to a species, rapidly accelerating pollen away from the plant by catapulting or exploding, and wind-induced mechanisms,

relying on aerodynamic forces that act directly on pollen grains, stamens and plants. Active mechanisms are not generally widespread and are perhaps specific innovations for wind pollination in sheltered environments. Many anemophilous plants have slender, exserted filaments that vibrate readily, and therefore the aeroelastic vibration model of Urzay et al. (2009) is a promising starting point for generalizing pollen release in these taxa. The influences of other aerodynamic forces such as drag, lift and shear acting directly on pollen grains as well as the effect of the bulk motion of plants have just barely been explored empirically and theoretically. The aerodynamic forces acting on catkins has not been investigated either. In each case, minimum threshold forces must be overcome that are directly related to properties of the anther and pollen grains and may be related to meteorology. Other than some generalizing statements about the nature of resistive forces, almost nothing is known. However, particle science and technology offers some promising leads. Whereas anemophilous plants may be optimized for aerodynamic pollen, the biophysical limits of wind pollination are simply unknown. Certainly aerodynamic pollen release occurs in some zoophilous species (i.e., *Brassica* sp., *Actinidia deliciosa*) (McCartney and Lacey, 1991; King and Ferguson, 1994), and therefore, dichotomous floral traits are probably not a good indication of stamen-wind interaction. Further study at the stamen and anther scales are needed to gain the insights into the mechanisms of pollen release.

Chapter 3

The Role of Vibration in Pollen Release by *Plantago lanceolata* L. (Plantaginaceae)

Summary

For most anemophilous species, there is little understanding of how the wind interacts with the stamen to release pollen grains. Using *Plantago lanceolata* we present empirical evidence that turbulence acts directly on stamens, causing resonance vibrations that release the grains. In the laboratory we show that stamens can be modeled as underdamped cantilever beams with elastic properties corresponding to the predicted ranges for turbulence-induced resonance vibrations. Exciting stamens near their natural frequency caused them to resonate, maximizing the amount of pollen released while minimizing the acceleration of the excitation at the time of release. There was a small effect of anther orientation on this acceleration with vibrations along the vertical axis shedding pollen more readily. Pollen release was episodic, with short bursts occurring at ever increasing accelerations for a given anther. The natural frequency increased with each episode due to the reduced mass of the anther, which increased the energy requirements for subsequent episodes or was perhaps due to differences in pollen adhesion forces within and among stamens. Observations under natural conditions in the field support the laboratory results and demonstrate that pollen is released from resonating stamens. It is possible that resonance vibrations of stamens may be a general mechanism facilitating pollen shedding in anemophilous angiosperms. Moreover, stamen properties such as damping ratio and flexural rigidity may provide useful measures for differentiating anemophilous from zoophilous species.

Introduction

Despite the ecological and economic relevance of wind pollination in forestry, agriculture, and human health, there is surprisingly little information on the mechanisms by which pollen is liberated from anthers into the airstream (Jackson and Lyford, 1999; Kuparinen, 2006; Martin et al., 2009; Martin et al., 2010). Indeed most studies model the process as continuous or discrete release hence oversimplifying a process that is known to be influenced by environmental conditions such as relative humidity and temperature (Kuparinen, 2006). Nonetheless several recent studies have characterized novel pollen release mechanisms that are likely restricted to a limited number of species with particular floral traits. For example, the stamens of *Morus alba* (Moraceae) and *Parietaria judaica* (Urticaceae) develop under increasing elastic tension that when released, catapults pollen from the anthers into the air column (Taylor et al., 2006; Franchi et al., 2007). In *Ambrosia* sp. (Asteraceae), clumps of pollen are swept from the anthers by the pistollidium and presented outside of the anthers directly to airflows (e.g., secondary pollen presentation) (Martin et al., 2009). Finally, *Ricinus communis* (Euphorbiaceae) has an explosive mechanism that propels pollen from the anther by the inversion and sudden reversion of the anther wall (Bianchini and Pacini, 1996; Hufford and Endress, 1989). Apart from the dramatic catapulting and exploding mechanisms, it appears that for the great majority of species, the wind mechanically stimulates pollen release (Niklas, 1985; Jackson and Lyford, 1999; Jones and Harrison, 2004; Taylor et al., 2002; Friedman and Harder, 2004; Taylor et al., 2004; Miguel et al., 2006).

It is likely that a pollen release mechanism would involve aerodynamic forces that act directly on stamens or on their supporting structures (e.g., catkins, scapes). It has been

suggested that turbulent kinetic energy from wind gusts may be transferred to the elastic motion of a stamen, accelerating it beyond the threshold that facilitates inertial pollen release (Niklas, 1992; Aylor et al., 2003; Urzay et al. 2009). This mechanism seems likely for anemophilous flowers that have unsheltered, flexible and exserted stamens which conspicuously oscillate even at low wind speeds (a behavior we have qualitatively observed in anemophilous species of Aceraceae, Gunneraceae, Plantaginaceae, Poaceae, and Ranunculaceae; pers. obs.; Niklas, 1992; Urzay et al., 2009). However, for the most part, this and other pollen release mechanism have not been examined.

A recent theoretical study proposed that the stamens of anemophilous plants can be treated as linear, isotropic cantilever beams with an apical load, which would facilitate their response to turbulence (Urzay et al., 2009). This idealization means that applying a force to the free end of the beam (e.g., wind loading) causes bending that increases linearly from the support regardless of the direction of the force. Further, a restoring force opposing the perturbation will be linearly proportional to the deflection of the beam and, after the removal of the perturbation, returns the beam to equilibrium. The dynamics of the relaxing beam are described by the harmonic oscillator which depends on the cyclic exchange rate of strain and kinetic energy called the natural frequency of vibration (f_n) and on the dissipation of energy from the system given by the damping ratio (ξ; Denny, 1988). For stamens, the natural frequency of vibration ($f_n = 10.9 - 35.5\ Hz$) and damping ratio ($\xi = 0.006 - 0.086$) were predicted by scaling arguments to be sufficiently low that turbulent eddies cause them to resonate with increasing amplitude and thus surpass the threshold required for the inertial release of pollen (Urzay et al., 2009). This prediction and the mechanical properties of stamens have not been measured

in anemophilous plants, nor have cantilever beams been shown to reliably approximate stamens. In addition there are other concerns related to the choice of parameter values for thresholds that were based on measurements from a small number of zoophilous plants, which are generally considered to have more pollen adhesion than anemophilous species (Urzay et al., 2009). Notwithstanding the limitations described above, it would be informative to determine whether stamens can be idealized as cantilever beams with a characteristic acceleration threshold for pollen release.

Plantago lanceolata L. (Plantaginaeceae) provides an ideal experimental system by which to examine the role of vibration in the release of pollen from stamens. Although there are reports of insect visitations during flowering, there is only a minor contribution of syrphid flies to its reproduction (Stelleman, 1984a), and there seems little doubt that the vast majority of fertilization events are due to wind pollination (Primack, 1978; Stelleman, 1984a). Unlike most anemophilous plants, flowering can be induced in the first three months of growth (Lacey, 1996). In addition, its small stature permits many individuals to be grown in a small area. Furthermore, flowering can be prolonged indefinitely by trimming back the scapes (personal observations). For mechanical testing, this species has the added benefit of having relatively large stamens which could be easily manipulated.

The goal of this study is, therefore to examine the mechanical response of stamens of *P. lanceolata* to vibration. If pollen is released via excitation by turbulent eddies, then stamens should respond to mechanical vibration as under-damped harmonic oscillators and pollen release is expected to occur at resonance. Furthermore, the anther orientation with respect to the axis of vibration may influence pollen release as pollen is less likely to

be obstructed by the anther wall if the motion is parallel to the stomium. The mechanical response of stamens was analyzed in the laboratory at various frequencies, amplitudes and orientations in order to determine the conditions for release. These data were then paired with field observations to assess if the proposed mechanism operates.

Materials and Methods

Biology and specimens of Plantago lanceolata

Plantago lanceolata (Plantaginaceae) is a cosmopolitan perennial herb that is established almost everywhere in mid- to high latitudes (Cavers et al., 1980). It produces a 2-8 cm long conical or cylindrical spike inflorescence on leafless scapes that extend up to 60 cm from a 3-40 cm basal diameter rosette. Although it is gynodioecious (Hyde and Williams, 1946), only hermaphrodites are examined here. The flowers are arranged spirally along the longitudinal axis of the spike at an angle of 60^{o} (Henderson, 1926). Each flower is approximately 3 mm in length and symmetrical in both axes with a centered pistil and 4 evenly spaced filaments (Henderson, 1926). As with many anemophilous plants, the corolla is severely reduced with respect to the length of the filaments (Primack, 1978). Two pollen lobes are joined to form a heart-shaped anther that hangs from a slender, horizontally exserted filament about 6 mm in length. The anther is versatile with respect to the filament and rotates or flaps freely at its end. Anther dehiscence is lengthwise at opposite ends (Hyde and Williams, 1946). Pollen production per anther is varied with accounts ranging from 11 908 ± 262.2 (mean ± SD) grains (Sharma et al., 1999) to as many as 20 500 ± 2200 (Hyde and Williams, 1946). On

average, each grain has a mass of 14.4×10^{-9} g and a diameter of 23×10^{-6} m (Jackson and Lyford, 1999).

To better understand the analysis, it is worth examining the development of the reproductive structures in some detail. At the onset of anthesis, the stigmas emerge from the still-erect corolla lobes as both spike and scape continue to elongate (Hyde and Williams, 1946). The majority of stigmas become receptive over the next few days, initiating the male reproductive stage. Under favourable weather conditions (e.g., warm, dry, sunny), the petals unfold, displaying the apices of the anthers inside. Early in the morning, the stamens unfurl from each flower, in horizontal rings starting at the base of the inflorescence and moving upwards. There are rarely more than 2 rings of stamens on any given day (pers. obs.). This process is temporarily suppressed by the onset of unfavourable conditions. The filaments are initially folded in two segments, a short and thin segment bearing the anther and a long, thick segment that is attached to the receptacle. Early in the morning, the filaments unfold and become turgid. In the next 4 stages, the stamens extend, dehisce and release pollen. In the first stage, the cells of the long segment elongate as the anther gradually becomes pendulate and versatile (*stage 1*; Fig 3.1A; Hyde and Williams, 1946). The filament then straightens as water is reabsorbed and evaporated from the anther. By midday, the anthers dehisce, initiating the pollen release stage (*stage 2*, Fig 3.1B). This can occur in as little as 5 minutes if conditions are favourable. Over the next few hours, the filaments oscillate conspicuously in even slight breezes (pers. obs.). The filaments maintain their turgor for several hours even after the majority of pollen is released (*stage 3*; Fig 3.1C). Gradually, the filament stiffness is

reduced, and the stamen wilt by the end of the same day that it dehisced (*stage 4*; Fig 3.1D; Young and Schmitt, 1995).

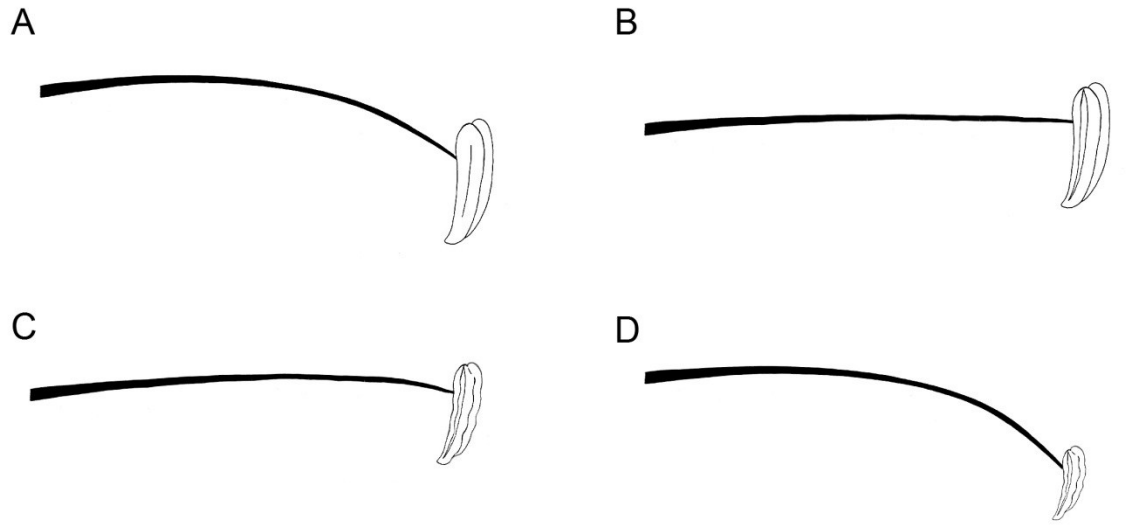

Figure 3.1: Stages of stamen development of *Plantago lanceolata* following anthesis. A) Fully extended filament, undehisced anther (*stage 1*). B) Turgid filament with newly dehisced anther (*stage 2*). C) Turgid filament with pollen depleted anther (*stage 3*). D) Wilted filament and anther (*stage 4*).

Specimens of *P. lanceolata* were grown from seeds obtained from Horizon Herbs (Williams, Oregon, USA). Seeds were individually germinated in 10 by 10 cm pots filled with potting soil in a growth chamber set to 16-hour 25^{o}C daylight intervals and 8-hour 21^{o}C dark intervals. Relative humidity varied between 50 and 60%. Once individuals had 4 leaves, the plants were fertilized weekly using a 10-20-10 liquid fertilizer. Flowering was observed after approximately 100 days of growth and all individuals flowered after 150 days. The plants were then transferred into a 21^{o}C, 50-60% relative humidity laboratory for analysis, where they were kept beneath a timer-controlled fluorescent lamp programmed at the same lighting interval as the growth chamber. In the laboratory anthesis was generally observed in the morning at approximately 7 am. By 9 am the vast majority of stamens were fully extended and dehiscence had begun. By the mid-afternoon, the majority of stamens had wilted, the rest of the inflorescence remaining

fully hydrated. Once flowering was completed, scapes were removed to promote further flowering.

The mechanical characteristics of stamens

Stamens with fully extended filaments and pendulate but pre-dehiscent anthers (*stage 1*) were selected for mechanical testing (n = 45). The use of non-ruptured anthers ensured that there was no mass lost by pollen release prior to and during the experiment, which may have compromised the results. *Stage 1* stamens also represented a boundary limit where the potential for pollen release was maximized. Between 8 and 9 am, when *stage 1* stamens were most abundant, a flower from a group of 30 plants was removed from an inflorescence using fine-tipped tweezers. The flower was then embedded at its base in an adhesive (Lepage Fun-Tak, Mississauga, Ontario, Canada), and mounted horizontally at the edge of an aluminum circular plate that was fixed to a vertically oriented SmartShaker Pro K2004E01 electrodynamic shaker (The Modal Shop, Cincinnati, Ohio, USA; e.g., Fig. 3.2A). Using tweezers, all but one stamen and the pistil were removed from the flower. The flower was discarded if any part of the procedure was thought to cause damage to the remaining stamen.

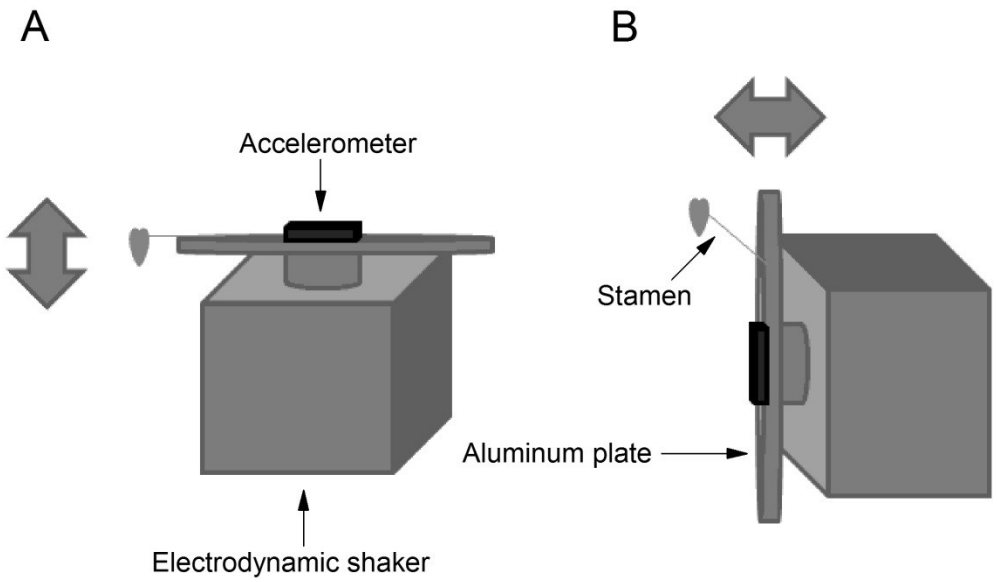

Figure 3.2: Schematic of electrodynamic shaker used to excite stamens of *Plantago lanceolata*. The system consists of a vibrating aluminum plate, an accelerometer and a stamen. Large arrows indicate the axis of vibration. A) Vibrations along the vertical axis. B) Vibrations along the horizontal axis.

To measure the dynamic properties of the stamen, a 4003A function generator (BK Precision, Yorba Linda, California, USA) excited the electrodynamic shaker, with a low-amplitude sinusoidal signal that increased from 8 to 42 Hz over a period of 5 seconds. The frequency range was based on preliminary observations that indicated that stamen resonance was likely to occur within this frequency range. It was important for the bandwidth to include the resonance frequency because it corresponds to the damped natural frequency of vibration, f_d (Rao and Gupta, 1999). The amplitude was just high enough to observe motion outside of resonance. The excitations were filmed through a Canon macro-lens fixed to a Casio Elixim FH25 digital camera focused perpendicular to the stamen. The video was recorded at 120 frames per second. A Phidget 1049 accelerometer (Phidgets inc., Calgary, Alberta, Canada) attached to the electrodynamic shaker captured its motion at 500 samples per second. Each stamen was vibrated for a total of 15 seconds (equivalent to 3 frequency sweep periods). The displacement-time series for the vertical motion of the filament was generated using Tracker Video Analysis

and Modeling software (Open Source Physics, http://www.compadre.org/osp/). The frequency spectrum was obtained by Fast Fourier Transform in OriginPro v8.6.0 Sr2 (OriginLabs, Northampton, Massachusetts, USA). The first mode in the spectrum was taken as the damped natural frequency of vibration. The damping ratio, ξ, was found by the half-power bandwidth method, $\xi = \frac{f_2 - f_1}{2f_d}$, where f_1 and f_2 corresponds to the frequencies on either side of the first mode where the amplitude is $\frac{1}{\sqrt{2}}$ of its maximum value (Rao and Gupta, 1999).

Deflection measurements were used to calculate expected values of f_n using the cantilever beam model (Niklas, 1992). Immediately following harmonic testing, the anther was plucked from the filament and placed in a weighed 0.2 ml microcentrifuge tube. The unloaded filament, reflexed upwards, and became straight. The difference in its displacement or deflection, Y, was measured in ImageJ from still images taken before and after the manipulation. The microcentrifuge tube was then weighed on a Mettler Toledo AX205 microbalance (sensitivity = 0.01 mg) and the mass of the anther, m_a, was determined by the difference method. The filament length, L, and width, W, were measured under light microscopy. The relationship between the flexural rigidity of the filament and the deflection is:

$$EI = \frac{m_a g L^3}{3Y} \qquad (3.1)$$

where g = acceleration due to gravity (King and Buchmann, 1995). The natural frequency of vibration is then related to the flexural rigidity by:

$$f_n = \frac{1}{2\pi}\sqrt{\frac{3EI}{m_a L^3}} \qquad (3.2a)$$

which is then reduced to:

$$f_n = \frac{1}{2\pi}\sqrt{\frac{g}{Y}} \qquad (3.2b)$$

The following standard assumptions about the filament were made for the preceding calculations: (1) the mass was negligible with respect to the anther mass; and (2) the cross-sectional area was constant. To determine whether or not the cantilever beam model reliably predicted the natural frequency of vibration, the correlation between the measured and calculated values of natural frequency of vibration was examined using ordinary least-squares regression. Significant effects were defined as $P < 0.05$.

Pollen shedding experiment

The minimum acceleration required for pollen release was determined for newly dehisced stamens (*stage 2*) using different excitation frequencies and directions of motion. Stamens were repeatedly excited to determine if there was variation in the pollen release threshold and in the amount of pollen released. The experiment was conducted between 9:00 and 10:00 am to ensure the availability of *stage 2* stamens. Stamens were mounted on the electrodynamic shaker using the procedure described above. Pollen was not displaced during the mounting procedure; otherwise the flower was discarded.

To test the hypotheses that the acceleration required for inertial pollen release depends on the frequency of vibration and the orientation of the anther with respect to the axis of vibration, stamens were excited either in the vertical or in the horizontal plane and

at a particular frequency. For vertical excitations, 50 stamens were individually vibrated at their natural frequency of vibration, at 60 Hz or at 120 Hz. The shaker was re-orientated for horizontal excitations (e.g., the top of the aluminum plate was placed normal to the vertical axis; Fig. 3.2B) and 30 stamens were individually vibrated either at their natural frequency or at 120 Hz. To find the natural frequency, the stamens were initially excited through a series of increasing frequencies and at very low amplitude to prevent pollen release. The natural frequency was re-evaluated whenever pollen release was observed. The excitation acceleration at the time of release was measured using the Phidget 1049 accelerometer for resonance excitations and a SEN-09332 adxl 193 accelerometer (SparkFun Electronics, Boulder, Colorado, USA) was used at higher frequency. For each treatment, an unused microscope slide coated with a thin gel layer of glycerin lubricant was held at a 45^{o} angle 1 cm from the anther. The excitation amplitude was then increased and muted when pollen was ejected from the anther onto the slide. In order to test the null hypotheses that there is only a single acceleration threshold, the procedure was repeated a maximum of 3 times. Multiple tests (termed "trials"; 2 or 3) were not ubiquitous since stamens could only be tested within the shaker's frequency-specific acceleration tolerances. The pollen slides were then examined under light microscopy and the number of grains ejected per trial was counted. For a subset of those slides belonging to the vertical / natural frequency of vibration treatment, the number of grains per pollen clump was counted into integer-bounded logarithm base-2 bins.

Multiple regression was used to determine the average effect of the excitation direction, frequency and trial number on the threshold acceleration and the amount of pollen released. Acceleration and number of pollen grains released were regressed against

5 dummy variables: (1) vertical (with horizontal as the reference group), (2) 60 Hz (with resonance frequency as the reference group), (3) 120 Hz (with resonance frequency as the reference group), (4) trial 2 (with trial 1 as the reference group), and (5) trial 3 (with trial 1 as the reference group). Finally, the effect of trial number on the mean of the $\log_2$ transformed clump size was analyzed using the Friedman test.

Field observations

Naturally occurring specimens of *Plantago lanceolata* were observed in the northwest section of a mowed field (Fig. 3.3) from September 9 – 13, 2012 at Delaware, Ontario, CA (42°55'N, 81°24'W, 224 m above MSL). The section had only been mowed once in early summer, and consisted of the focal species, long grasses, and ~1 m high shrubs. The northern and western perimeters of the section were sheltered by a mixture of coniferous and deciduous trees ranging in height from ~4.0 to 15.0 m. An 81000 ultrasonic anemometer (R.M. Young, Traverse City, MI, USA) was positioned on a tripod at a height of 2.0 m at the center of the section. Orthogonal wind velocity measurements in 3 axes (*u, v, w*) and temperature were sampled digitally by a SmartReader Plus 7 data logger (ACR Systems, Surrey, BC, CA) at a frequency of 25 Hz. The +*v* direction was north-facing and represented the horizontal datum (0°), whereas the +*u* and +*w* directions were west- and up-facing, respectively.

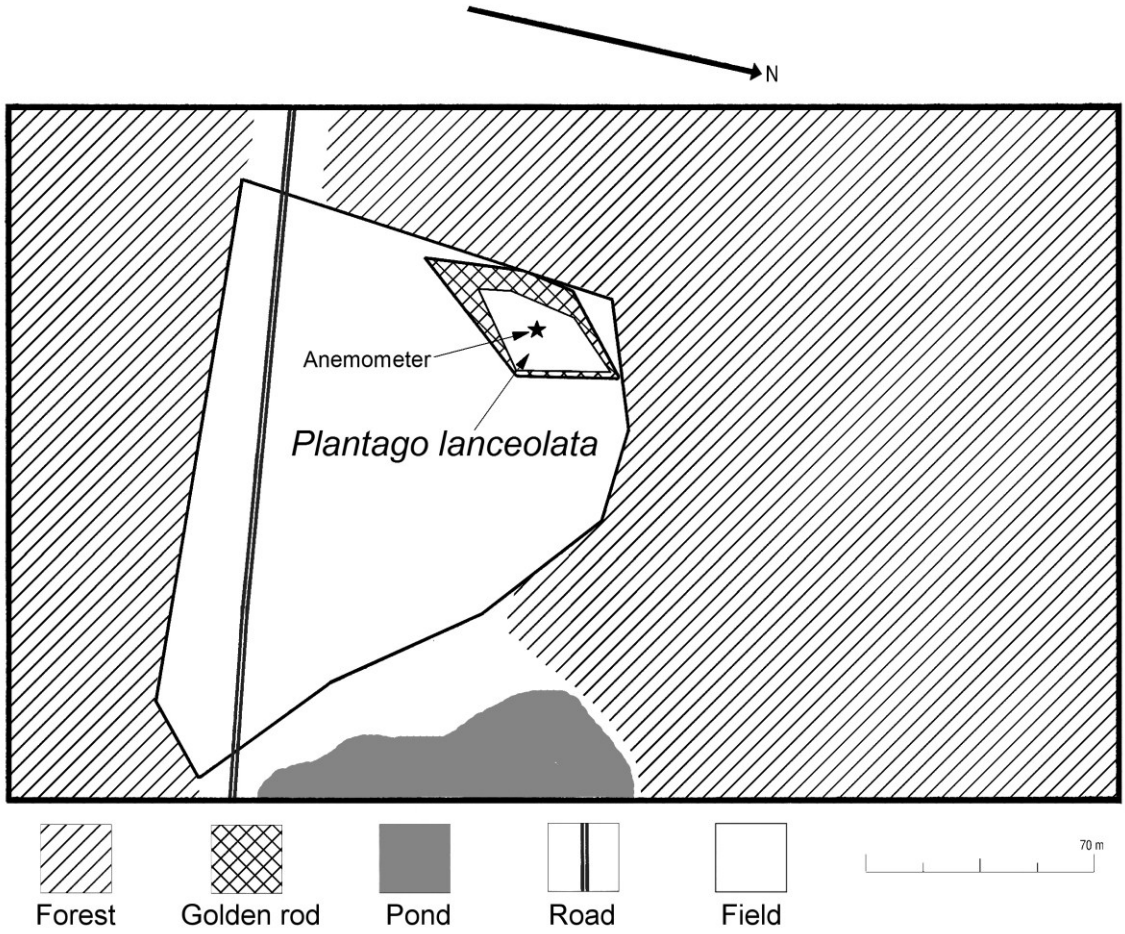

Figure 3.3: Map of field site in Southwestern Ontario.

On sunny or moderately cloudy days, stamens were filmed using the high speed camera system described above (sampling frequency = 120 Hz), using the inbuilt 20× zoom lens. Each specimen was located within a horizontal radius of 2.0 m from the anemometer. Specimens were selected based on whether or not it was convenient to film in their vicinity. Selected plants were not adjacent to any shrubs or long grasses. Using a wind vane located in one corner of the section, the camera and tripod were positioned downwind of a focal plant to minimize interference with the flow, and at least 20.0 cm from the stamen. The camera was positioned as close to the stamens as possible so that at least one stamen was in focus. To prevent the wind from moving the stamens out of

focus, the scape was fixed to a thin wooden stake using masking tape, 2.0 cm below the spike.

Most of the plants observed had fully extended (*stage 1*) stamens by 9:00 a.m, and were usually covered in dew. On sunny warm days, the moisture evaporated quickly and dehiscence soon followed. Cloudy conditions delayed evaporation and dehiscence by one or two hours. Regardless of conditions, by noon, the vast majority of stamens had dehisced and were mostly depleted of pollen. However, the filaments maintained their turgor well into the afternoon, which is similar to what was observed in the laboratory.

Between 10:00 am and 12:00 pm, *stage 1* to *3* stamens were filmed and wind velocity was sampled over 9 minute intervals. Later, videos were separated for processing into one minute segments and displacement time series were produced for the single most visible stamen in each video using the video analysis method described above. Stamen displacement fluctuations (y') and wind velocity fluctuations (u', v', w') were calculated using the formula $x' = x_i - \bar{x}$, where $x_i =$ the instantaneous measurement and $\bar{x} =$ the time averaged value and were normalized for comparison using the formula $\frac{x_i - \min(x)}{\max(x) - \min(x)}$ where $x_i =$ the value to be normalized and $x =$ is the distribution to which it belongs. Fourier analysis was used to evaluate the temporal periodicity and frequency distribution of energy for the normalized fluctuations. Power spectra were generated via a rectangular window in OriginPro v8.6.0 Sr2 with a cutoff frequency (e.g., $Nyquist\ frequency = \frac{sampling\ rate}{2}$) of 60 Hz for stamen displacements and 13 Hz for wind velocities. The spectral density method used by this software is based on the periodogram, which estimates power as the amplitude squared (see: Anonymous, 2013).

Results

Laboratory experiments

The time-varying sinusoidal oscillations of the electrodynamic shaker caused the stamens to vibrate in the vertical axis with increasing frequency and amplitude. Invariably, the displacement increased in the vertical axis to a maximum and then relaxed (Fig. 3.4 inset). The damped natural frequency of vibration and the damping ratio were extracted from the corresponding amplitude spectrum (Fig. 3.4). On average, stamens resonated at f_d = 20 ± 4 (average ± standard deviation) Hz (n = 45) and were under-damped, $\xi = 0.051 \pm 0.009$.

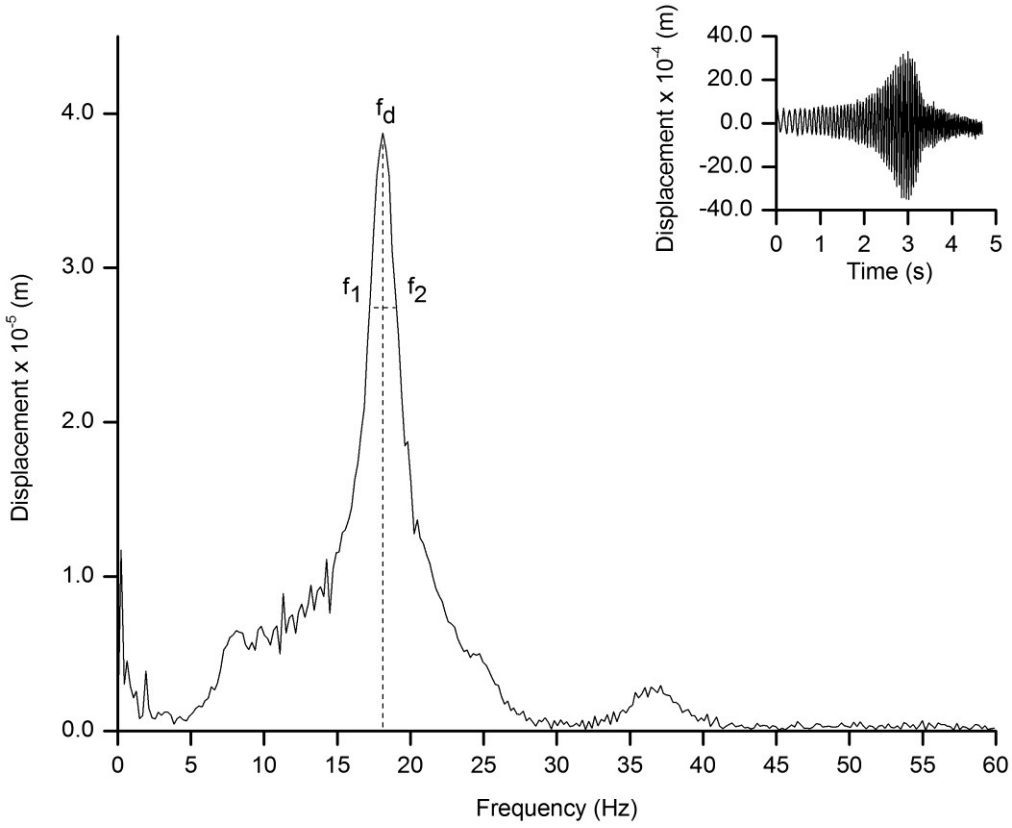

Figure 3.4: Representative displacement spectrum for an undehisced *Plantago lanceolata* stamen. The inset represents the corresponding displacement time-series. f_d = damped natural frequency of vibration; f_1, f_2 = frequencies at $\frac{1}{\sqrt{2}}$ of the maximum amplitude, used in the half-power bandwidth method.

The removal of the anthers from the filaments resulted in a vertical deflection, Y = $1.0 \pm 0.4 \times 10^{-3}$ m (n = 37). Of 8 stamens excluded from this analysis, 2 were permanently deformed and 6 were damaged by the experimental procedure. The average anther mass and filament length were $m_a = 3.2 \pm 0.8 \times 10^{-7}$ kg and $L = 6.5 \pm 1 \times 10^{-3}$ m, respectively. The natural frequency of vibration and the deflection were both weakly correlated with the filament length ($r^2 = 0.090$, $F_{1,35} = 4.7$, P = 0.040 for f_n vs. L; $r^2 = 0.14$, $F_{1,35} = 57$, P = 0.010 for Y vs. L) but not with the anther mass ($r^2 = 0.020$, $F_{1,35} = 1.7$, P = 0.21 for f_n vs. m_a; $r^2 = 0.13$, $F_{1,35} = 2.2$, P = 0.15 for Y vs. m_a). Flexural rigidity was calculated for each stamen, resulting in an average $EI = 3.0 \pm 2.0 \times 10^{-10}$ Nm^2. From these measurements, theoretical values for the natural frequency of vibration were calculated by equation (2) and averaged as $f_{expected} = 17 \pm 3$ Hz. The calculated frequency value significantly predicted the measured frequency with bias(Fig. 3.5, $r^2 = 0.56$, $F_{1,35} = 47$, $P < 0.001$) (i.e., via t-tests the intercept was significantly greater than 0 t(35)=1.3, P =0.21).

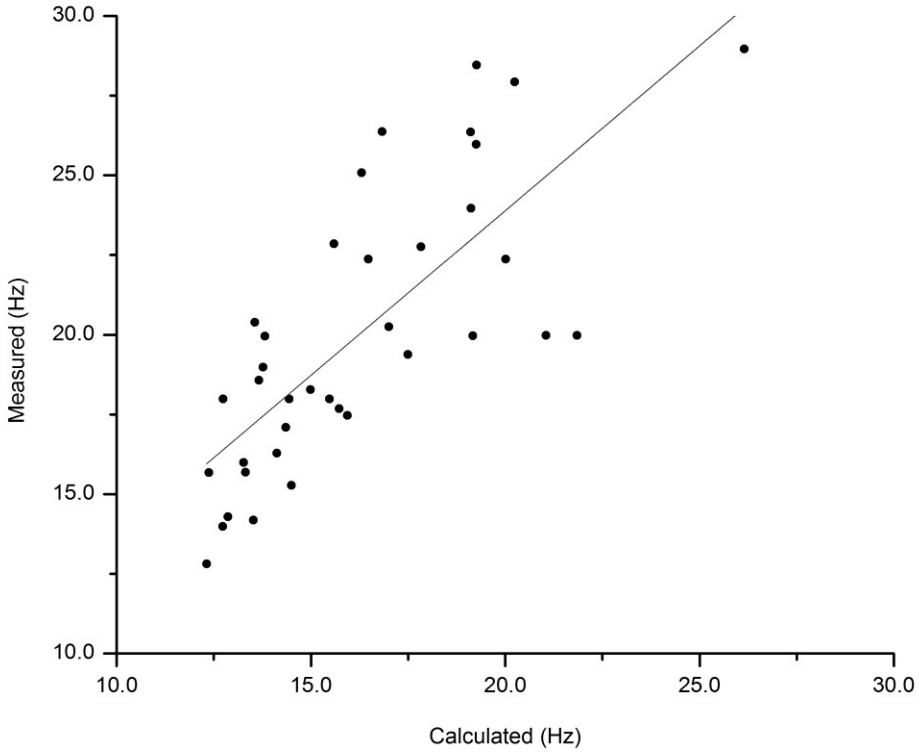

Figure 3.5: Measured vs. calculated natural frequency for undehisced anthers (slope = 1.03 ± 0.15; intercept = 3.20 ± 2.50; r^2=0.56, P<0.05; mean ± SE. Intercept is significantly greater than 0).

Pollen was released from *stage 2* dehisced anthers in multiple discrete bursts. At resonance, these events were preceded by a slight elliptical whirling motion of the filament in the vertical axis that was most noticeable only at high accelerations (e.g., close to the threshold). For all frequencies, there was shaking (e.g., rotation and tilt) of the anther that had no noticeable periodicity. This motion began near the threshold and became increasingly chaotic with amplitude. This motion also made it impossible to track stamen displacements from video. Therefore, it was not possible to analyze the dynamic response of dehisced stamens. The acceleration required for the release of pollen almost always increased between trials irrespective of the treatment (Fig. 3.6). Significant models resulted from the multiple regressions (Table 3.1) on acceleration (R^2 = 0.75,

$F_{5,476} = 290$, $P < 0.001$) and on the number of grains released ($R^2 = 0.21$, $F_{5,511} = 28$, $P < 0.001$). Summarizing Table 3.1, the acceleration required to eject pollen from anthers was greater for/at: (1) vertical excitations than for horizontal excitations; (2) excitations of 60 Hz than for excitations at resonance; (3) excitations of 120 Hz than for excitations at resonance; (4) second bursts than for first bursts; and (5) third bursts than for first bursts. Further, the amount of pollen released during each trial was: (1) greater for vertical excitations than for horizontal excitations; and (2) greater for excitations at resonance than for 120 Hz excitations. No significant differences in the amount of pollen released were found for: (1) 60 Hz excitations relative to resonance excitations; (2) between the second and first trials; and (3) between the third and first trials. The force required for the vibratory release of pollen based on an average pollen grain mass of 1.44 x 10^{-11} kg was 0.1 – 0.2 nN at resonance and 1.3 – 2.1 nN at 120 Hz ($F = ma$).

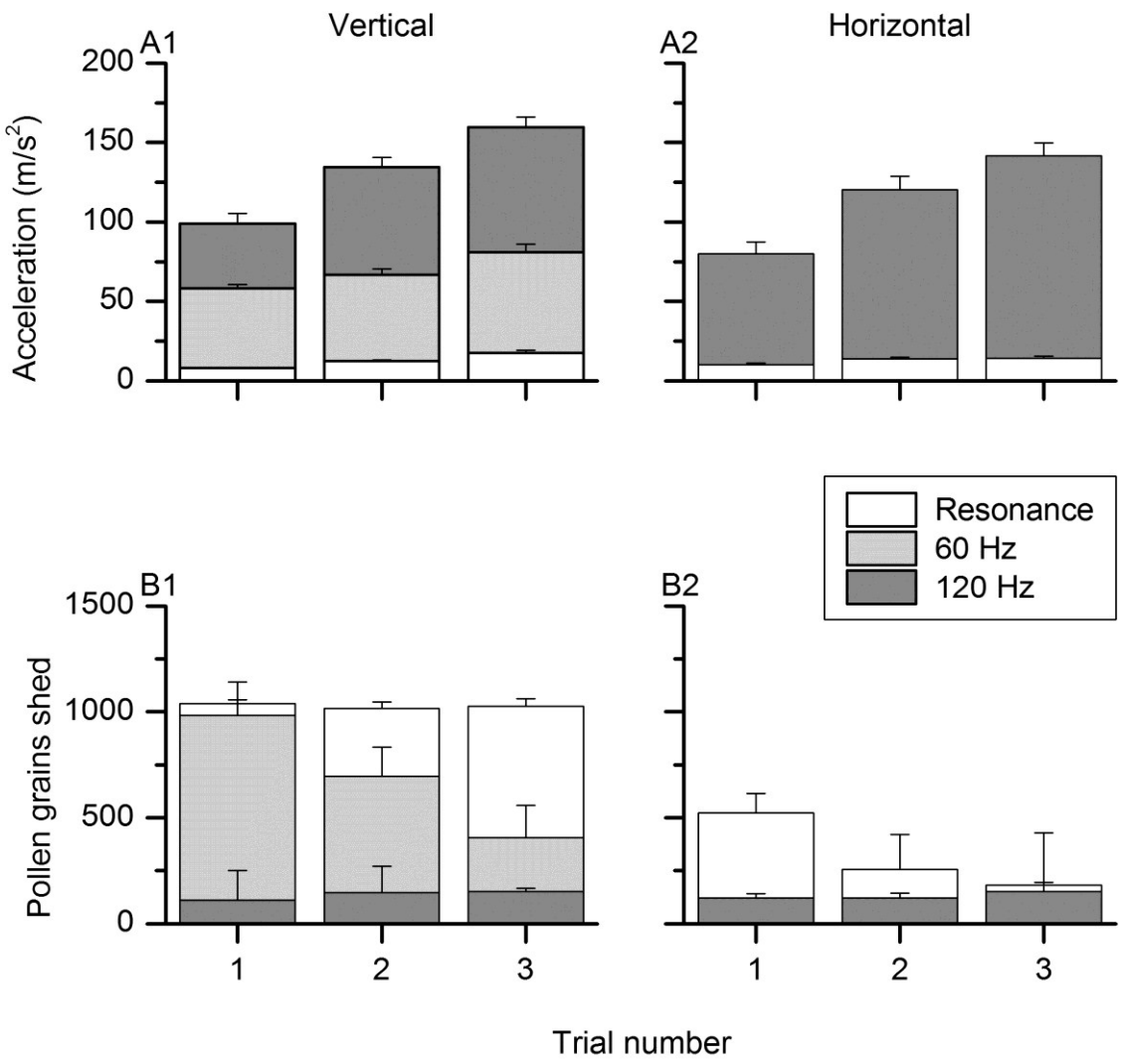

Figure 3.6: Summary results of the pollen shedding experiment in *Plantago lanceolata*, showing the simultaneous effects on release acceleration and number of grains shed of 3 treatments: (1) axis of vibration, (2) frequency of vibration and (3) repeated measures. A1, B1 show stamens vibrated in the vertical axis. A2, B2 show stamens vibrated in the horizontal axis. Frequency treatment is represented by the tone of each bar. Bar rise to their average value (e.g. they are not cumulative). Abscissia represents sequential trials (repeated measures) of stamens. Error bars represent the standard deviation.

Table 3.1: Results of dummy variable regression of pollen release experiment.

		Details of multiple regression model			Model summary	
Dependent variable	Independent variable	b	Std. Error	P	R^2	P
Acceleration	vertical vs. horizontal	17	3	< 0.01**	0.75	< 0.01**
	60 Hz vs. resonance	62	5	< 0.01**		
	120 Hz vs. resonance	120	3	< 0.01**		
	trial 2 vs. trial 1	18	4	< 0.01**		
	trial 3 vs. trial 1	36	4	< 0.01**		
	Constant	-14	4	< 0.01**		
No. pollen grains	vertical vs. horizontal	330	69	< 0.01**	0.22	< 0.01**
	60 Hz vs. resonance	-12	85	0.89		
	120 Hz vs. resonance	-590	68	< 0.01**		
	trial 2 vs. trial 1	-33	69	0.63		
	trial 3 vs. trial 1	-20	75	0.79		
	Constant	6.0×10^2	75	< 0.01**		

** P< 0.05

The natural frequency of vibration almost always increased after pollen release events. Since the sequence of trials occurred in short succession, it is unlikely that the frequency was affected by changes to filament turgor pressure between trials. It is also unlikely that vibration treatments had significant effects (e.g., plastic deformation) on the material properties of stamens (e.g., flexural rigidity) since the frequency did not change between successions of sinusoidal frequency sweeps of *stage 1* stamens. Given the mass relation in equation (2a), it is most likely that the change in frequency resulted from the change in anther mass following a release event. Indeed, the relative change in frequency, $d_r = 100\frac{\Delta f}{f_0}$ where Δf = the absolute change in frequency and f_0 = the initial frequency, was significantly correlated with the total number of pollen grains released after a

sequence of 3 trials (Fig. 3.7, $r^2 = 0.68$, $F_{1,133} = 111$, $P < 0.001$). Finally, no significant differences were found among the three sequential ejection events in the $\log_2$ transformed mean clump size (Fig. 3.8, $X^2_2 = 3.8$, $P = 0.16$).

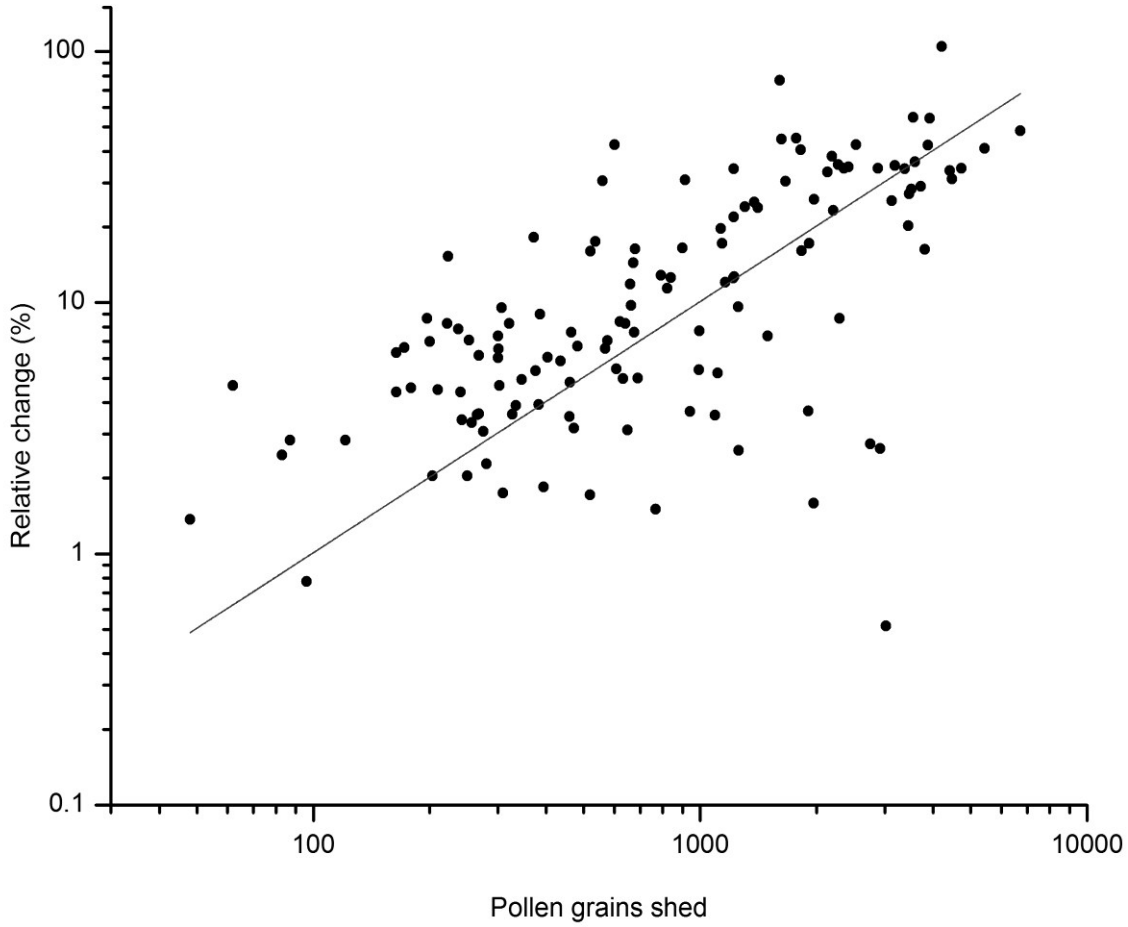

Figure 3.7: Relative change in natural frequency as a function of number of pollen grains released (slope = 0.0100 ± 0.0006; $r^2 = 0.68$, $P < 0.001$).

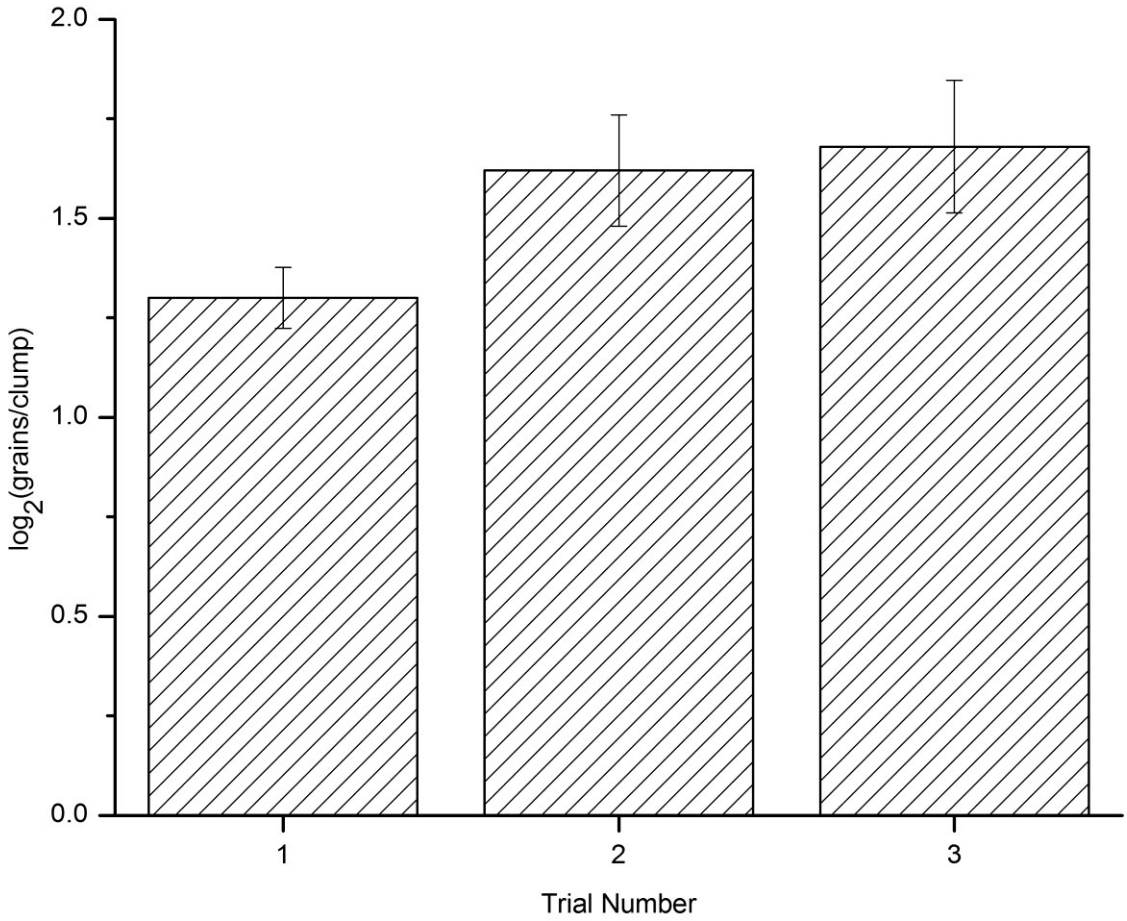

Figure 3.8: Average pollen clump size for 3 consecutive pollen release trials; n = 9.

Field observations

Displacement curves were generated for four stamens from different plants. Summary statistics of the stamen characteristics, average conditions and turbulence conditions are provided in Table 3.2. The samples and their corresponding meteorological conditions are labeled A through D. Stamen A was undehisced and at *stage 1,* whereas Stamens B-D corresponded generally to stamens between *stages 2* and *3* (dehisced with a large proportion of pollen removed). Each periodogram plot in Fig. 3.9 represents the ensemble average of 9 spectra from each 1 minute video segment. The magnitude at each frequency represents a proportion of the total variance described by a

sinusoidal function at that frequency. Therefore, the greatest amplitude displacements were generally associated with low frequency oscillations. Despite the overall decline in power with frequency, stamens A and C had narrow spikes at higher frequencies, whereas stamen B had a wider bulge (Fig. 3.9 arrows). No obvious spike was seen within the frequency limit of stamen D but, as with the other stamens, the rate of power reduction started to decline for frequencies above ~10 Hz. Unlike the other stamens, stamen A had 2 large peaks, the first reaching a maximum at 2.6 Hz (no arrow shown) and the second at 16.5 Hz. As the upper 2 cm of the scape and spike was free to oscillate, it is likely that the peak at 2.6 Hz corresponds to the bulk motion of the inflorescence as was seen in the spectra of inflorescence displacement fluctuations (note only one peak was observed; not shown).

Table 3.2: Summary statistics from field observations.

Stamen		Average conditions														Turbulent conditions			
Stamen ID/ Sampling Interval	Date and time	H	y_{cv}	T	Θ	$\overline{ws}$	$\bar{u}$	$\bar{v}$	$\bar{w}$	u_{max}	v_{max}	w_{max}	u_{min}	v_{min}	w_{min}	I_{ws}	I_u	I_v	I_w
A	10/09/12 12:46	0.27	0.23	18.5	153	0.26	0.22	0.12	-0.05	3.40	1.74	1.00	-2.12	-2.11	-1.10	0.16	0.30	0.29	0.25
B	11/09/12 10:52	0.29	0.33	20.6	178	0.04	0.02	-0.03	-0.02	3.50	2.48	1.56	-3.26	-3.00	-2.16	0.14	0.27	0.28	0.17
C	11/09/12 11:30	0.16	0.22	21.5	176	0.87	0.00	-0.87	0.04	3.02	1.60	1.56	-2.65	-5.26	-2.31	0.13	0.27	0.22	0.17
D	13/09/12 10:40	0.31	0.32	25.0	187	0.32	0.06	-0.31	-0.01	2.72	1.10	0.77	-1.34	-2.23	-1.30	0.14	0.39	0.23	0.17

* Wind velocity was measured at a height of 2 m
A, B, C, D: Refers to a unique stamen and its sampling interval
H: Stamen height; y_{cv}: Coefficient of variation of stamen displacement fluctuations (m)
T: Temperature; Θ: Clockwise angle with respect to north (^{o}C)
$\overline{ws}$: Average wind speed; $\bar{u}, \bar{v}, \bar{w}$: Average one-dimensional wind velocities (m/s)
$u_{max}, v_{max}, w_{max}$: Maximum wind velocities (m/s)
$u_{min}, v_{min}, w_{min}$: Minimum wind velocities (m/s)
I_{ws}: Three-dimensional turbulence intensity
I_u, I_v, I_w: One-dimensional turbulence intensities

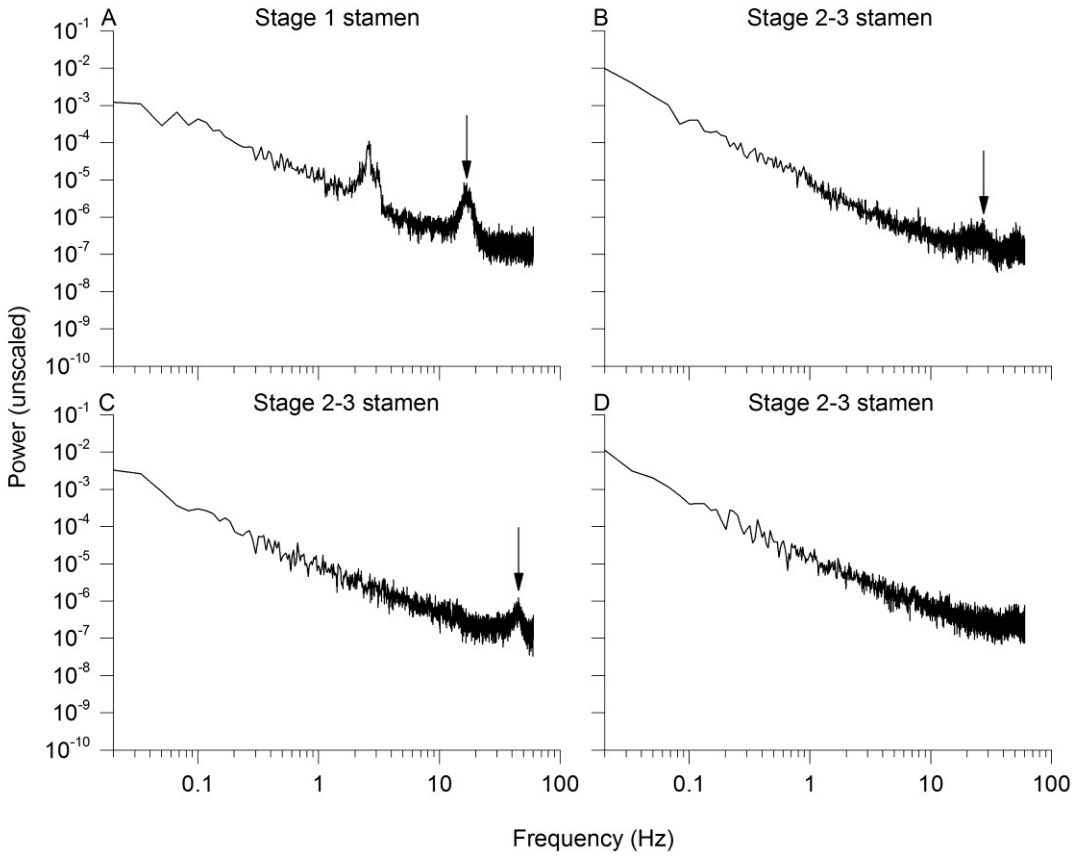

Figure 3.9: Ensemble average power spectra of normalized *Plantago lanceolata* stamen fluctuations. Each panel shows spectra for a different stamen. Arrows indicate resonance frequencies of stamens.

The spectra of the normalized wind speed fluctuation are provided in Figure 3.10. Wind conditions did not vary greatly between directions or sampling intervals. The average speed was always below 1.0 m/s and blew from the southeast (Table 3.2). Although the average speed was ~ 0.0 m/s during sampling interval B, the variability was consistent with the other intervals. The frequency distribution of power was also similar among directions, with an average slope of -1.64 ± 0.01 (based on the log transformed data), which is reasonably close to the -5/3 slope expected for atmospheric turbulence (Wyngaard, 2010). By comparison with stamen A, the power reduction rate for stamen displacement fluctuations was less steep (slope = -1.14) than for wind speed fluctuations,

suggesting a more platykurtic energy distribution for stamens. The sudden narrow-bandwidth peaks in power are consistent with harmonic excitation around the natural frequency, since resonating stamens store elastic energy which amplifies their dynamic response in relation to an excitation (Denny, 1988). Moreover, the second peak in stamen A occurs at a frequency well within the range of natural frequencies measured in the laboratory, and the higher magnitude peak frequencies for stamens B and C are consistent with magnitudes measured for dehisced stamens in the lab (recall that the natural frequency increased whenever pollen was removed from the anther; e.g., Figure 3.7).

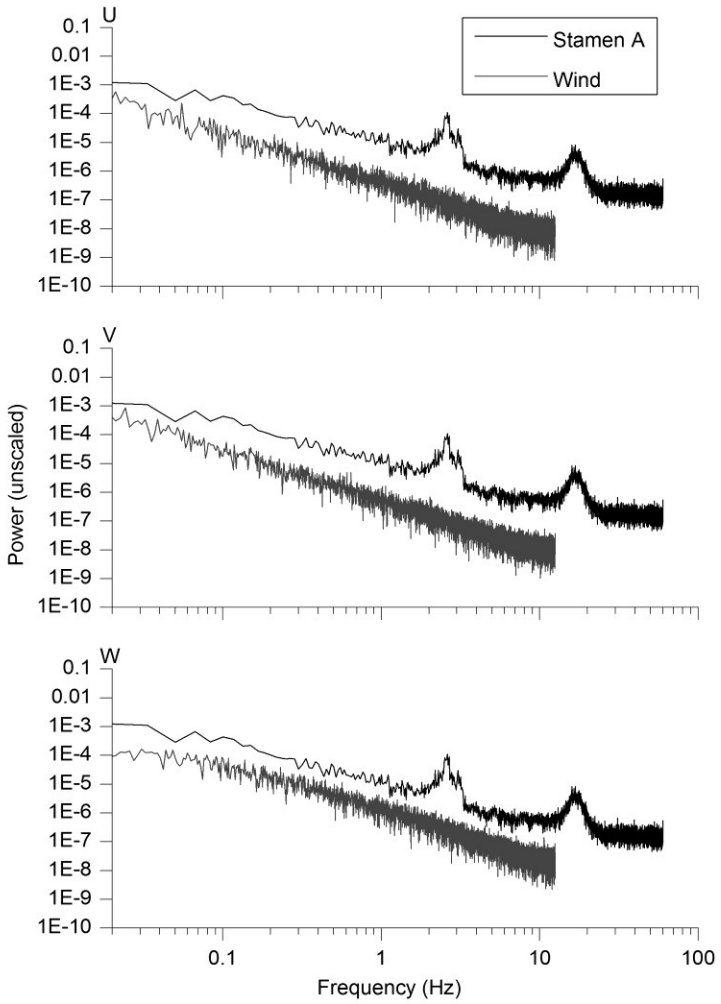

Figure 3.10: Power spectra of normalized wind speed fluctuations measured at a height of 2 m. Panels each represent the ensemble averages of four samples measured over 9 minute intervals. (*u*) Longitudinal axis, (*v*) lateral axis, and (*w*) vertical axis. The spectrum for stamen A (Fig. 9A) is superimposed for illustrative purposes. The range in frequency varies between wind speed and stamen fluctuations due to differences in sampling rate.

Importantly, the wind-induced elastic motion of stamen B coincided with pollen release as shown in Figure 3.11 (see right hand-most panel, $t = 0.025$ s). From this series of images, the stamen recovered (Fig. 3.11, $t = 0.025$ s) from a perturbation (Fig. 3.11, $t = 0.000 – 0.017$ s) of $d = 0.002$ m in $t = 0.008$ s, corresponding to a velocity of $v = 0.25$ m/s. Its acceleration was calculated by $a = \frac{2v^2}{gd}$, giving 63 m/s^2. The frequency was then

calculated by $\frac{v}{\pi D}$, giving 40 Hz, corresponding to a 15% difference from the peak value in Figure 3.9C.

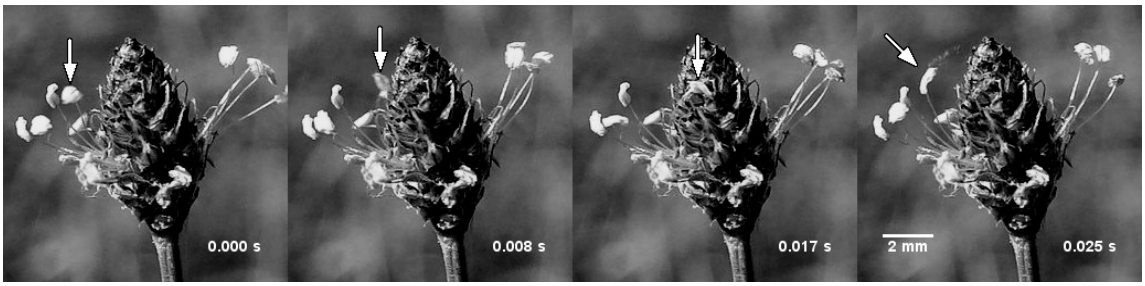

Figure 3.11: Vibration induced pollen shedding: corresponds to stamen C in Fig. 9C. The arrow tracks the motion of a single stamen over time. t = 0.000 s – 0.017 s shows the perturbation. t = 0.025 s shows the stamen returning to its equilibrium position and pollen release (t = 0.0025 s).

Discussion

The cantilever beam model provided a reasonable approximation for stamens of *Plantago lanceolata*. The measured properties of natural frequency and damping ratio were consistent with the theoretical ranges predicted to generate resonance vibrations by wind excitations. This response was confirmed in a natural population where pollen release was observed from a resonating stamen. In the laboratory, pollen release was episodic, in short bursts, occurring at ever increasing acceleration thresholds. Resonance vibrations minimized the threshold vibrations and maximized the quantity of pollen released. The force required to release pollen was also consistent across treatments with the measurement used in the analysis of Urzay et al. (2009).

Wind causes the stamen to resonate, which if the amplitude of the vibration is of sufficient magnitude to exceed the resistance forces on the pollen grains, then ejection of at least some of the grains within the dehisced anther must occur. Turbulent airflows are composed of a wide spectrum of eddies, oscillating over a broad range of frequencies

(Blevins, 2009). These various-sized eddies interact with structures, such as cantilever beams, immersed in the flow, applying time-varying dynamic loads to their surfaces. The kinetic energy content of each eddy depends on its frequency, and declines according to a power-law relationship to very small eddies dominated by viscosity. If there is enough energy in the spectrum near the natural frequency of a structure, it will resonate with increasing amplitude that depends on the strength of the gust, static and dynamic properties of the structure, and time. As a result, low-intensity wind gusts can generate dynamic loads on structures resulting in much larger deflections than those generated by static loads at the same mean wind speed. This phenomenon is found in the stems of plants and it often leads to stem failure and plant lodging (Flesch and Grant, 1992; Sterling et al., 2003). Niklas (1992) speculated that this mechanism should also operate in anemophilous plants, and we think that it will prove to be the dominant mode of pollen release for this group. Urzay et al. (2009) elaborated this prediction of Niklas using physical scaling arguments. To the best of our knowledge, the current paper is the first to examine this pollen shedding mechanism empirically.

A less likely way in which flow-induced vibration of beams might cause pollen shedding is via the alternating low-pressure vortices that detach from the downstream face of the structure (i.e., von Karman vortex street; Niklas, 1992). The resulting alternating sideways force can cause the beam to vibrate at a frequency equal to the vortex shedding frequency (Denny, 1988). The structure may resonate if this frequency is close to the natural frequency of the beam. It is possible to make an order of magnitude estimate of frequency based on its proportionality to the ratio of wind speed to beam diameter ($f \propto \frac{U}{D}$, where $U =$ wind speed and $D =$ diameter). For $D \sim 1 \times 10^{-4}$ m, typical

of filaments, and $U = 1$ m/s, $f \sim 10\,000$ Hz, which suggests that vortex shedding is unlikely to be an important cause of stamen vibration. A determination of the Reynolds number ($Re = UD/\nu$, where ν is the kinematic viscosity) associated with stamen filament supports this as vortex streets occur when $Re > 80$ (Schlichting and Gersten, 2000), which is greater than the range determined in this study (i.e., $6.4 < Re < 64$).

The particularly low value of damping ratio ($\xi = 0.051$) of *P. lanceolata* is of interest as very large amplitudes are expected in resonating beams as $\xi \to 0$ (Denny, 1988). In turn, amplitude is important because it is not enough for stamens to merely resonate; they must also cross a threshold that facilitates the inertial release of pollen. The response of a cantilever beam excited by a periodic force depends not only on the natural frequency but on properties such as flexural rigidity, EI, and the damping ratio, ξ (Denny, 1988). For high values of either parameter, the excitation may not contain sufficient energy to reach the threshold.

Unfortunately, few studies of the elastic properties of plant organs have addressed stamens and these are all limited to zoophilous species. Furthermore, these studies do not include a full range of measurements for comparison with *Plantango lanceolata* (i.e., no study of a zoophilous stamens has simultaneously measured f_n, ξ and EI, Table 3.3). Natural frequency is the most commonly measured parameter, ranging from 12 Hz to 108 Hz in the species examined (King and Lengoc, 1993; King and Buchmann, 1995; King and Buchmann, 1996). Damping ratio, previously measured only for stamens of the zoophilous *Solanum laciniatum* ($\xi = 0.13$, $f_n \sim 35$ Hz), was twice that of *P. lanceolata* (King and Buchmann, 1996). Flexural rigidity values for the zoophilous *Rhododendron augustinii* and *Rhododendron maddenii* were estimated from King and Buchmann (1995)

using equation (1) (i.e., $EI \sim 5.4 \times 10^{-7}$ nm^2, $f_n \sim 108$ Hz); this is three orders of magnitude greater than with *P. lanceolata*. We speculate that if the vibration release mechanism is common, anemophilous species generally will have much lower values of stamen EI and ξ, and therefore such differences may serve diagnostically to differentiate between wind and insects as vectors. That is, it is reasonable to suggest that there will be a large degree of aeroelastic specialization in stamens selected for efficient release by wind-induced vibration (anemophiles) *or* for a very low rate of wind-induced release from zoophilous stamens.

Table 3.3: Comparison of measured *P. lanceolata* vibration parameters with published values for putative zoophilous species.

Species	Vector	f_n	ξ	EI
Plantago lanceolata	Wind	20	0.051	3.0×-10^{-10}
Actinidia deliciosa[1]	Bees	12	--	--
Rhododendron spp.[2]	Bees	108	--	5.38×10^{-7}
Solanum laciniatum[3]	Bees	35	0.13	--

[1] from King and Ferguson (1993)
[2] from King and Buchmann (1995)
[3] from King and Buchmann (1996)
Vector: Putative pollination vector
f_n: Natural frequency of vibration (Hz)
ξ: Damping ratio
EI: Flexural rigidity (nm^2)

We showed in the field that vibration of *P. lanceolata* stamens could induce shedding. The response of a beam to wind loading is considered in terms of a background and resonance response. The background response is equivalent to the effect of the fluctuating component of the airflow when the natural frequency is much higher than the frequencies of the energy-containing eddies (Blevins, 2009). The resonance response is

an additional amplification of the background response caused by dynamic response to excitation near the natural frequency. The spectra of 3 of the 4 stamens examined were consistent with having both background and resonance components (Fig. 3.9A-C, Fig. 3.10). This suggests that the motion of the stamen does not merely reflect wind velocity fluctuations. Instead, the motion is best described as a combination of internal (e.g., effect of resonance) and external (e.g., effect of wind) responses. A similar set of responses is also found in the bulk motion of herbaceous stems of cultigens such as corn (Flesch and Grant, 1992) and wheat (Sterling et al., 2003).

Why then was there no resonance response in the spectrum of the 4th stamen (Fig. 3.9D)? One explanation may be that the natural frequency was greater than the Nyquist or cutoff frequency of the sampler (i.e., half of the sampling frequency). As shown in Figure 3.7, the loss of pollen caused an increase in the natural frequency and therefore, a more depleted anther would have a higher natural frequency. The pollen content of the stamen in question could have been so low that the digital video could not capture its resonance response. Similarly, the frequency could have been so high that there was not enough energy in the wind spectrum to cause the stamen to resonate. The stamen may also have failed to resonate because its elastic properties were compromised. Stamens eventually wilt and flutter in the wind. Therefore, there must be a temporal limit to their elasticity. A more thorough analysis is needed to evaluate these effects. Interestingly, in the video in question, the stamen did not appear to be any less turgid than any other stamens examined, nor was there any noticeable difference in the quality of its motion.

Pollen release in the laboratory appeared to be related to excitations at the resonance frequency. The importance of resonance is probably related to the

amplification of the anther acceleration relative to the excitation amplitude, reaching a maximum at resonance. Consequently, for a given input of energy, the acceleration of pollen grains is also greatest at resonance. For the pollen grains to reach the substantially higher acceleration threshold at 120 Hz, resonating stamen would have had to be amplified by about a factor of 10. It should be noted that for excitations above the natural frequency of a cantilever beam, the acceleration and inertia decay monotonically from the maximum to zero (Denny, 1988). At high frequencies, the pollen grains would have negligible inertia and the inertial release of pollen would no longer be possible. Since the frequency response of stamens was not measured, it is not possible to determine if the release force was equivalent for the different excitation frequencies. Nevertheless, the kinetic energy of the excitation, based on the squared ratio of amplitude to frequency (King and Buchmann, 1995) required to release pollen, was smaller for resonating stamens. Optimizing stamen response, in terms of energy input, for resonance would be advantageous in a turbulence-initiated vibration regime where the excitation energy associated with a particular frequency decreases with frequency.

The cause of differential pollen shedding in relation to the axis of vibration is not clear. One may assume that when stamens are excited in the horizontal axis pollen is more easily released because it is accelerating towards the stomium. Although excitations in the horizontal axis required a lower acceleration to release pollen, fewer pollen grains were released. Part of the solution may lie with the versatile anthers which rotates the stomium away from the axis of motion. Further study is needed to determine if there is an interaction between these two motions and if there is an effect on the minimum acceleration for release and amount of pollen released. A similar “versatile” anther-

filament coupling is found in the anemophilous *Halophytum ameghinoi* (Halophytaceae). Pozner and Cocucci (2006) hypothesize that rocking of the anther pushes pollen towards the stomium of *H. ameghinoi* and out of the anther. However, this has not been substantiated with experiments or observations. Versatile anthers are also found in many zoophilous species and are known to have functional roles in pollen release, distributing pollen directly onto the bodies of flying animals such as birds, bats and moths (D'Arcy, 1996).

As there were multiple bursts of pollen, there must be a distribution of thresholds for the inertial release of pollen within each anther; i.e. there must be variation in the forces resisting the acceleration of the pollen. Although there is only a rudimentary understanding of these forces in anthers, it is probable that the intra-granular tapetum-derived adhesives (e.g., pollen glues such as pollenkitt) typical of zoophiles are central to pollen release (Harder and Johnson, 2008). King and Lengoc (1993) and King and Ferguson (1994) noted multiple bursts of pollen from the stamens of the buzz-pollinated *Actinidia deliosa*, found intra-anther variation in the distribution of tapetal fluid, and argued that vibration caused the severance of interstitial bridges of pollen glue, liberating some pollen for release.

Although it is primarily wind pollinated, pollenkitt is present in the anthers of *P. lanceolata*, and while it is possible that vibration does indeed induce variation in adhesion, other mechanisms may be responsible. Conversely, the variation may be driven by differential drying, with more exposed pollen drying more quickly. King and Ferguson (1994) found that the quantity of tapetal fluid decreased over time, presumably by evaporation in a gradient from the stomium to the locular wall. In any case, there may

be other important forms of pollen adhesion and cohesion including mechanical interlocking, electrostatic forces and the van-der-Waals force (Barbosa-Canovas, 2005).

If pollenkitt is unevenly distributed within the anthers of *P. lanceolata*, we expect not merely staggering of the shedding, but also a non-uniform distribution of post-release pollen clump sizes. At release, different-sized clumps would have different inertias resulting from their unequal masses. With *P. lanceolata* under conditions that are unfavourable for wind pollination (e.g., for individuals occurring in sheltered environments), it has been shown that syrphid flies contributed importantly to the reproduction (Stelleman, 1984a). Pollen clumping was greatest in this population compared with individuals from open, more turbulent environments, suggesting that pollenkitt is either more abundant in the sheltered population or that it is more viscous. Stelleman (1984a) hypothesized that pollenkitt retention in sheltered environments was a means to ensure that an adequate supply of pollen remains on the anther for insect pollinators. Conversely, flies may have had more opportunity to sample the pollen in sheltered environments simply because both the drying rate and the likelihood of shedding via resonant vibration would undoubtedly be lessened with the speed often near 0.

While the quantity of pollenkitt may serve evolutionarily to decrease the probability that post-dehiscence release is accomplished by the wind, pollenkitt-driven staggering may simply be a dispensing mechanism. If all pollen is released at the same time from a variety of stamens on a single plant, those grains will have a highly correlated probability (similar direction and speed) of reaching any particular stigma; staggering increases the number of stigmas that might be reached by the plant. The

stamens of many anemophilous plants share a number of characteristics in common including exsertion and flexibility, which, in light of the present results, suggest adaptation for turbulence-initiated vibratory pollen release. There remain many unanswered questions regarding the exact nature of the process. Further studies should, for example, investigate the effects of varying meteorological conditions on the strength of resistive forces and on the pollen release rate. This would not only improve the realism of dispersal models but would make clear whether or not pollenkitt has been selected as a trait to limit the release of pollen from the anther. A more serious description of the role played by versatile anthers and the effect of wind direction in pollen release is also required. On a final note, considering that most flowers are chasmogomous and exposed to the atmosphere, they should be affected to varying degrees by turbulence. Plants that rely only on biotic vectors should evolve to avoid pollen losses to wind since these grains would be of little reproductive value. Therefore, zoophilous plants should have mechanisms to control both the character of surrounding turbulence and biomechanical properties of stamens reducing the vibratory response. Indeed, as we saw, there is some evidence that zoophilous plants have higher damping ratios and flexural rigidities. Further, it is considered part of the classic syndromes of zootic- and wind-pollinated plants that the former tend to have more closed corollas (Faegri and Pijl, 1979) so that the anthers experience much lower wind speeds. Ambophilous species, that is those pollinated by both wind and animal vectors, ought to have intermediate traits in this respect, conserving some fraction of the pollen for visitors while releasing some to wind gusts. There are clear distinctions between anemophilous and zoophilous flowers that are attributed to the varying physical requirements of their

pollination vectors (Niklas, 1985). Evaluation of these evolutionary speculations requires that we reframe the discussion of floral evolution in terms of biomechanical properties. We think there are quantitative gradients of properties such as damping ratio and flexural rigidity that will serve to discriminate between vectors, will eventually replace the qualitative traits used in contemporary descriptions of pollination syndromes, and will contribute importantly to our understanding of the evolution of flowers.

Chapter 4

Using the Probability Distribution of Pollen Clump Sizes to Predict the Pollination Vector

This chapter resulted from collaborations with David F. Greene, Josef D. Ackerman, Peter G. Kevan and Erika Nardone. All authors contributed to the ideas of the manuscript. D.F.G, J.D.A. and P.G.K. contributed to the writing, and E.N. contributed to the planning and execution of the methodology.

Summary

Although a constellation of floral traits, the pollination syndrome, is used to predict the pollination system of a plant, there has been little attempt to advance a simple, reliable quantitative measure. Here we consider the probability distribution of pollen grain clump sizes as a quantitative predictor. A standardized procedure for generating pollen clump size distributions, via the random disaggregation of clumps, is introduced and we hypothesize it will produce a lognormal distribution. We examined this hypothesis intraspecifically using the ambophilous *Plantago lanceolata*, and then interspecifically with 31 putative anemophilous and zoophilous species. Using the first and second moments of the lognormal distribution, we tested the hypothesis that the distribution of clump sizes is correlated with the pollination vector. As expected, almost all samples tested exhibited a strong right skew. A small majority, 57%, of *P. lanceolata* samples fit the lognormal distribution, whereas among species the distribution was fit by about 75% of the species. In samples that did not fit the lognormal it was because of a too-large fraction of singletons. The mean and standard deviation of the lognormal distribution, in addition to a third parameter, the proportion of singletons, all separated

the samples by vector with the mean outperforming the other two metrics. While our results indicate that clump size may be a promising quantitative measure, we call for a more careful study of the effects of other factors on clump size such as relative humidity and time since anther dehiscence, as well as for a standardized methodology.

Introduction

The diversification and specialization of flowers has been driven by the interaction of floral traits and pollinators (Fenster et al., 2004; van der Niet and Johnson, 2012). Indeed, similarity in the evolutionary response of flowers to a particular pollination vector has given rise to the concept of "pollination syndromes"; i.e., a suite of floral traits specific to each vector, in many cases representing convergent evolution (Faegri and van der Pijl, 1979; Ackerman, 2000; Ollerton et al., 2009). Although this concept has been criticized, it is still the common basis for inferring pollination systems (Ollerton et al. 2009). However, field experiments often reveal a complexity of pollination systems (Ollerton, 1996; Wasser, 1998; Johnson and Steiner, 2000) whereby plants such as *Plantago lanceolata* (Stelleman, 1984a) and *Cocos nucifera* (Melendez-Ramirez et al., 2004) may exhibit strictly anemophilous or zoophilous syndromes, respectively, yet rely on both vectors – i.e., ambophily (Stelleman, 1984b; Friedman and Barrett, 2009). Field observations can also be problematic as there may be spatial and temporal asymmetries in the proportions of the most frequent or efficient pollination vectors within or among populations (Waser et al., 1996; Sahli and Conner, 2006; Olessen et al., 2008).

Several functional approaches have been used to infer pollination vector from the quantification of floral traits. For example, a strongly male-biased reproductive output is often considered advantageous for wind pollination as a form of bet-hedging because the probability of any one grain reaching a stigma is so poor (Whitehead, 1969; Ackerman, 2000; Friedman and Barrett, 2009), and thus the pollen-to-ovule ratio is usually much higher for anemophilous plants than for zoophiles (Cruden, 1977; Michalski and Durka, 2009). At the other extreme, autogamous plants have far less pollen and consequently much lower pollen-to-ovule ratios than anemophilous plants (Cruden, 2000).The settling velocity of pollen grains is another trait that has been considered diagnostic of the pollination vector (Hall and Walter, 2011) with lower settling velocities, which lead to longer dispersal distances, considered advantageous in anemophily (Di-Giovanni et al., 1995; Di-Giovanni et al., 1996; Ackerman, 2000). However, no explicit relationship between pollen settling velocity and pollination vector has been found (Hall and Walter, 2011), which may be due to a small sample size or could indicate that other factors are responsible. For example, a smaller grain size permits the production of a larger number of grains for the same reproductive effort and may not be related to pollen dispersal (Ackerman, 2000; Hall and Walter, 2011).

The tendency of pollen to clump is related to the settling velocity argument described above, as pollen aggregates should have higher settling velocities than solitary grains (Niklas, 1985; Di-Giovanni et al, 1995; Jackson and Lyford, 1999; Martin et al., 2009), and thus aggregation has also been used as a basis for inferring the pollination vector (Stelleman, 1984a; Vroege and Stelleman, 1990; Hall and Walter, 2011). Clumped pollen may be disadvantageous for anemophiles during anthesis as a greater force would

be required to remove aggregates than singletons from the anther into the air column. It should be noted, however, that pollen liberation was enhanced by clumping in *Ambrosia artemisiifolia,* which is the only study to examine the distribution of pollen clump sizes at the time of release, of which we are aware (Martin et al., 2009). Whereas its role in anemophily is unclear, pollen clumping is often advantageous in biotic pollination (depending on the aggregation mechanisms present; cf., Harder and Johnson, 2008) as it can improve siring success by increasing the adhesion of pollen to visitors (via viscous compounds (pollenkitt) or threads (viscin), reducing pollen loss during grooming (via threaded pollen or pollinia), and delivering multiple pollen grains to the stigmas.

Hall and Walter (2011) argued that the magnitude of clumping, determined by the proportion of solitary pollen grains (their "aggregation index"), provides a measure to distinguish between anemophilous and zoophilous species. However, the general use of the aggregation index for determining pollination vectors is unclear, given their small sample and because the clump size distribution may be sensitive to sampling methodology. For example, *A. artemisiifolia* (ragweed; anemophilous) tends to have very clumped pollen shortly after dehiscence (Martin et al., 2009); subsequently, the clumps rapidly disaggregate by turbulence in dry air over a distance of only a few meters. Similarly, the pollen of *Solanum laciniatum* (kangaroo apple; zoophilous) is initially released as clumps when bumblebees vibrate the anthers at high frequency, but is almost completely disaggregated when captured in still air on microscope slides placed a short distance from the flower (King and Buchman, 1996). Given the occurrence of high clumping and the near-complete disaggregation of pollen clumps soon after release, the correct categorization of these species, based on the measurement of aggregation index,

would depend on when and how their pollen was sampled. This speaks to the need for a better technique for discriminating between pollen vectors using morphological criteria.

We expect that the temporal sequence of disaggregation events, being a multiplicative process, should result in a right skewed distribution of pollen clump sizes that becomes lognormal with time (King, 1981). In nature, these disaggregation events are a result of pollenkitt drying, turbulent air, or contact with animal pollinators (Stelleman, 1984a; Pacini, 2000; King and Buchman, 1996; Martin et al., 2009). There are three situations however where the probability of pollen clump sizes would be right skewed but not necessarily log-normal: (1) disaggregation is not random with respect to clump size; (2) there has been too little time for the disaggregation process to operate; and (3) too much time has elapsed, so that singletons (the lower limit for the disaggregation process) become very numerous.

The purpose of the following study is, therefore, to examine whether or not the moments of a lognormal distribution (e.g., mean and standard deviation) can be used to discriminate between pollen vectors. We examine this question intraspecifically in an ambophilous species, *Plantago lanceolata* (with the vector designation based on field observations), where one would expect an intermediate amount of clumping. Those results are then contrasted with an interspecific examination across anemophilous and zoophilous species whose pollen vector characterization is based on pollination syndromes.

Materials and Methods

Intraspecific analysis of Plantago lanceolata

Plants of *Plantago lanceolata*, an ambophile (Stelleman, 1984a), were grown in 10 by 10 cm pots from seeds obtained from Horizon Herbs (Williams, Oregon, USA). Flowering was induced over 3 months in a growth chamber using 16-hour daylight intervals at 25^{o}C and 8 hour dark intervals at 21^{o}C. When flowering was observed in April 2012, the plants were transferred to a laboratory at Concordia University in Montreal, Quebec, where they were kept beneath a timer-controlled fluorescent lamp programmed at the same lightning schedule as noted above. Relative humidity in both environments varied between 50 and 60%.

We applied standardized forces to pollen samples that would initiate the disaggregation process. These methods were used to produce "sprinkling images" of pollen dispersed on microscope slides, and then the resulting distributions of pollen clump sizes were measured. The first of these methods vibrated pollen from 30 anthers of *P. lanceolata*. Shortly after dehiscence, typically between 9 and 10 am, flowers were removed from the inflorescence by plucking them at the receptacle base by using fine-tipped forceps. We were careful to not dislodge pollen from the anthers. The bases of these flowers were then embedded in an adhesive (Lepage Fun-Tak, Mississauga, Ontario, Canada). Each was then mounted horizontally onto a vertically oriented SmartShaker Pro K2004E01 electrodynamic shaker (Cincinnati, Ohio, USA). Three of the 4 stamens and the carpel were removed from the flower using forceps. A microscope slide coated with silicon grease was then placed 1 cm from the anther at a 45^{o} angle. A

BK Precision 4003A signal generator (Yorba Linda, California, USA) was used to vibrate the shaker sinusoidally through increasing frequencies at low amplitude until the stamen began to resonate. The excitation was then amplified until the resonating stamen ejected pollen onto the microscope slide. The falling grains were captured on the microscope slide and examined under light microscopy to generate a frequency distribution of pollen clump size (grains per clump). Frequencies of pollen grains per clump were grouped into 11 integer bounded base-2 logarithmic bins.

Interspecific analysis

We quantified the disaggregation of pollen sampled from flowers with intact anthers from 23 species (Table 1) that were in bloom between November 27 and December 2, 2010 around the Pró-Mata Research and Nature Conservation Center in Rio Grande do Sul, Brazil. All plants were identified to the species level, with the exception of three Poaceae, which were classified as separate species based on morphological and phenological differences. The specimens were kept in water on a lab bench beneath an incandescent lamp until dehiscence could be observed with a hand lens (usually within 2 hr). The designation of pollination vectors were based to some degree on observations at the field station but were mainly inferred from the macroscopic floral traits of specimens (i.e. pollination syndromes). Although we observed the frequent visitation of syrphid flies on the flowers of *Plantago major*, we have included it with the anemophilous plants since, to our knowledge, no study has shown ambophily in this species.

We followed the technique of Stelleman (1984a) and Ackerman and Kevan (2005) to produce sprinkling images of pollen dispersed on microscope slides. Briefly,

pollen from the newly dehisced anther was shaken through a 1.91 cm diameter hole bored lengthwise through a 30 cm aluminium cylinder in which an acrylic disk was placed at half the cylinder length (see Ackerman and Kevan, 2005).The cylinder was then inverted by 180^{o} and lowered to 1 mm above a microscope slide coated with a thin layer of silicon grease. A steel 1.40 cm diameter steel ball bearing was dropped through the top of the cylinder where it collided with the acrylic block and the shock dislodged the pollen on its underside. The falling grains were trapped on the microscope slide and examined under light microscopy to generate a frequency distribution of pollen clump size (grains per clump) as described above. Clumps were defined as sets of pollen grains in physical contact.

Statistical analysis

To assess if disaggregated pollen follow a lognormal distribution, the intra- and interspecific clump size distributions were compared to a lognormal distribution using the Kolmogorov-Smirnov goodness-of-fit test. Data from Hall and Walter (2011) were included in this analysis (4 anemophilous and 4 zoophilous species). Because their largest pollen clump size bin was unbounded (>100 grains per clump), we assumed that no clump would exceed 2048 grains – an exceedingly rare upper bound for our observations in Rio Grande do Sul – in order to calculate the statistical moments of the lognormal distributions.

We also used contingency tables to examine the hypothesis that the distribution of clump sizes was independent of the pollination vector (anemophilous and zoophilous). To test this hypothesis, we grouped the data from Rio Grande do Sul into 4 pollen clump size

classes to ensure that each cell had a minimum of 5 observations, satisfying the assumptions of the χ^2 test.

The 'aggregation index' (*AI*), a minimum estimate of the proportion of solitary grains used by Hall and Walter (2011) to quantify clumping, was calculated for each distribution by dividing the number of solitary grains (f_s) by the sum of each of the 11 pollen clump size bin's frequency (f_i) multiplied by its lower bound (l_i; $AI = fs / \sum_{i=1}^{11} f_i l_i$). We examined if there were similarities in the first two statistical moments (i.e., mean and standard deviation) of the lognormal distribution of pollen clump size and *AI* between anemophilous and zoophilous species by separate Mann-Whitney U tests. Least-squares linear regression was used to examine the relationship between the moments of the lognormal distribution of pollen clump size and *AI* for each pollination vector. Data from Hall and Walter (2011) were combined with the species studied here and also tested separately.

Results

The pollen released from *Plantago lanceolata* was found to clump with 172 ± 102 (average ± standard deviation) pollen clumps per anther (n = 30 individuals examined; a total of 5165 pollen clumps examined). The distributions of pollen clump sizes ranged from singletons to 64 pollen grains per clump in a markedly right skewed fashion (skewness, g_1, = 1.51) with a frequency of 81 ± 55 for the singletons and 0.03 ± 0.18 for the largest clump size (Fig. 4.1). The mean clump size was 2.64 ± 1.96 pollen grains per clump (i.e., 1.4 ± 0.97 $\log_2$(pollen grains per clump)) and *AI* (proportion of singletons)

was 0.21 (Table 4.1). A small majority (e.g., 17 of 30 flowers or 57%) of the pollen clump distributions was found to fit a lognormal distribution ($X^2 < \frac{1.36}{\sqrt{n}}$, Kolmogorov-Smirnov goodness-of-fit tests). The remaining flowers had pollen clump size distributions that were right skewed but not lognormal.

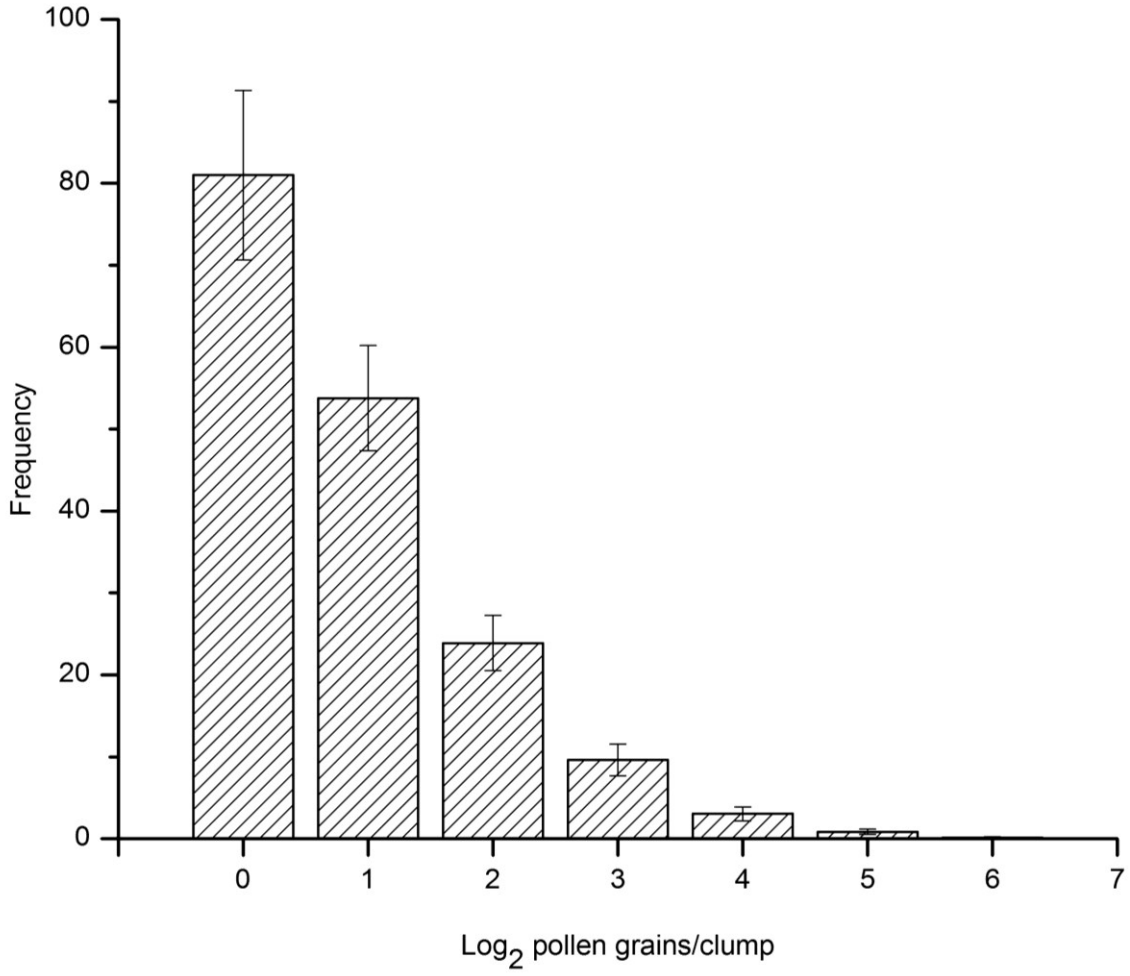

Figure 4.1: Ensemble average (mean ± SE) of $\log_2$ (pollen clump size) for *Plantago lanceolata*. Bars are centered on bin lower bounds (bin width = 1).

Pollen clumping was also found in anemophilous (n = 5) and zoophilous species (n = 17), although it was more extensive in the latter, extending to clump sizes of 1024 pollen grains per clump (vs. 512 among the anemophiles) (Fig 4.2). The distributions were also right skewed (Table 1), especially among the anemophilous species where

frequencies of 204 ± 277 pollen grains per clump were found among singletons versus 0.20 ± 0.45 pollen grains per clump for the largest pollen clumps. The difference among bin frequencies was much lower among the zoophilous species with a maximum of 21 ± 32 pollen grains for singletons. Not surprisingly, the mean clump size was less for anemophilous species with the inclusion of the data from Hall and Walter (2011) with 1.55 ± 1.61 pollen grains per clump (n = 8; i.e., 0.63 ± 0.69 $\log_2$(pollen grains per clump)) and *AI*= 0.65 for the anemophilous species, and 8.11 ± 3.41 pollen grains per clump (n = 22; i.e., 3.02 ± 1.77 $\log_2$(pollen grains per clump)) and *AI* was 0.06 for the zoophilous species (Table 1). Approximately, three quarters of the anemophilous (75%) and zoophilous (73%) species had pollen clump size distributions that followed a lognormal distribution ($X^2<\frac{1.36}{\sqrt{n}}$, Kolmogorov-Smirnov goodness-of-fit tests; Table 1).

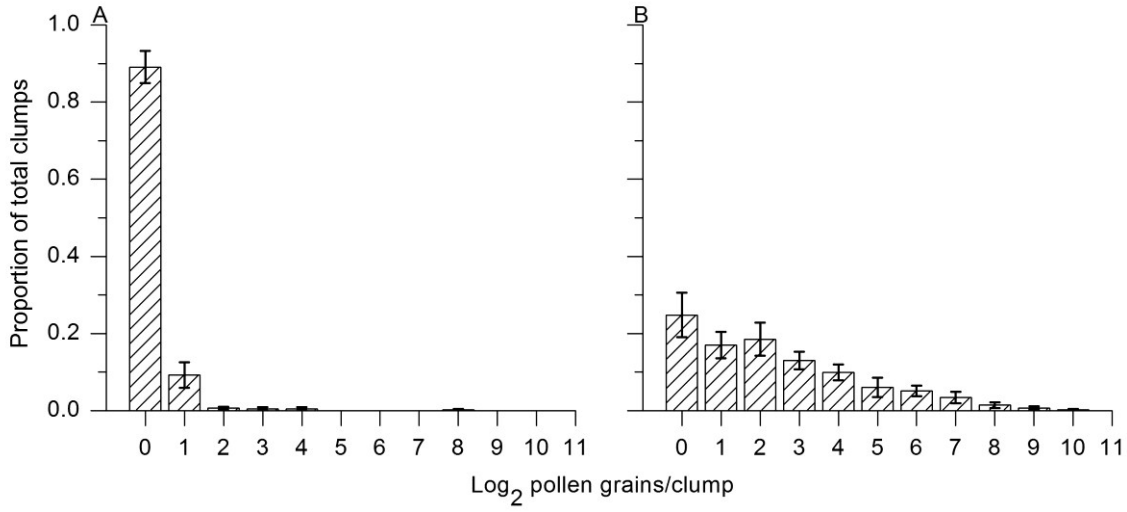

Figure 4.2: Average proportion (mean ± SE) of $\log_2$ (pollen clump size) for anemophilous species (A) and zoophilous (B) species studied in Brazil and presented in Table 1. Bars are centered on bin lower bounds (bin width = 1).

Table 4.1: Statistics for plant species organized by pollination vector.

Pollination Vector	Species	No. clumps	$\bar{X}$	SD	g_1	*AI*	*D*
Anemophilous	*Araucaria cunninghamii*[+#]	113	0.59	0.85	10.39	0.58	0.232
	Pinus tecunumanii[+#]	68	0.69	1.27	5.43	0.52	0.283
	Casuarina cunninghamiana[+]	296	0.62	1.19	5.93	0.54	0.282**
	Gunnera manicata	50	0.5	0.00	--	1.00	--
	Plantago major	90	0.93	1.15	4.13	0.17	0.263**
	Poaceae species 1	822	0.66	0.39	2.29	0.73	0.040
	Poaceae species 2	102	0.65	0.36	1.98	0.95	0.014
	Poaceae species3	119	0.53	0.16	6.03	0.74	0.024
	Zea mays[+]	92	0.48	0.82	10.74	0.65	0.229
	MEAN:		**0.63**	**0.69**	**5.87**	**0.65**	
Zoophilous	*Cycas revoluta*[+#]	75	1.51	2.46	0.61	0.08	0.307
	Lepidozamia peroffskyana[+#]	246	0.99	1.80	2.59	0.25	0.309**
	Baccharis trimera	10	2.2	2.31	0.69	0.05	0.298
	Begonia cucullata	23	5.11	1.41	0.22	0.00	0.053**
	Buckinghamia celsissima[+]	59	1.31	1.98	1.75	0.14	0.253
	Coccocypselum condalia	13	2.04	1.05	0.11	0.04	0.053
	Fuchsia regia	40	1.98	1.45	0.76	0.06	0.193
	Hymenocallislittoralis[+]	26	2.71	2.62	0.56	0.05	0.178
	Ilex paraguariensis	22	3.05	1.53	0.86	0.00	0.610**
	Jacobina carnea	15	2.97	2.72	0.55	0.02	0.239
	Lupinus magnistipulatus	77	2.62	1.35	1.24	0.23	0.102
	Lupinus reitzii	71	1.19	1.44	2.59	0.00	0.271
	Mutisia speciosa	72	1.85	1.90	1.48	0.08	0.190
	Passiflora caerulea	66	2.89	2.56	0.81	0.01	0.152
	Roupala rhombifolia	136	1.31	1.15	1.45	0.21	0.179
	Senecio brasiliensis	485	2.15	1.30	0.60	0.04	0.048

	Sinningia warmingii	93	5.89	1.94	0.61	0.00	0.154**
	Sisyrinchium palmifolium	43	6.2	1.79	-0.06	0.00	0.068**
	Sisyrinchium sellowianum	99	1.35	1.31	2.23	0.19	0.160
	Solanum variabile	40	2.4	0.93	-0.38	0.03	0.158
	Trixis lessingii	79	2.99	1.13	-0.25	0.01	0.054
	Vriesia platynema	88	3.49	1.58	2.64	0.00	0.225**
	MEAN:		**3.02**	**1.77**		**0.06**	
Ambophilous	*Plantago lanceolata*	172	1.4	0.97	1.51	0.21	

$\overline{X}$, SD, g_1, AI and D refer to the mean and the standard deviation of $\log_2$(pollen clump size), the skewness, the aggregation index, and the Kolmogorov-Smirnov D statistic respectively.
[+]from Hall and Walter (2011).
[#]Gymnosperms.
** *P<0.05*.

As indicated above, the distribution of pollen clumps was dependent on the pollination vector (X^2_3= 132.51, P < 0.05; N = 23) in that clump sizes were larger among the zoophilous species (4.39 and 3.89 times larger for mean and standard deviation, respectively; Fig. 4.2; Table 1). In addition, there were significant differences between the means and standard deviations, respectively, of the $\log_2$-transformed data for anemophilous and zoophilous species (Mann-Whitney U = 0.0, i.e., mean clumping sizes all tended to be larger in the zoophiles, P = 0.001; and U = 3.5, P = 0.002 for standard deviation. Similarly, the aggregation index (*AI*) of Hall and Walter (2011) was 11.5 times larger for anemophilous than zoophilous species, and differed significantly between vectors (U = 3.0, P = 0.002). A significant linear relationship was found between *AI* and the mean and standard deviation of the logarithms of clump size (r^2 = 0.40, n = 32, P < 0.001, for *AI* vs. mean; r^2 = 0.52, n = 32, P < 0.001, for *AI* vs. standard deviation; Fig 4.3a and b). There overall trend was similar when the analysis was repeated using separate data sets (i.e., r^2 = 0.34, n = 23, P = 0.002 for *AI* vs. mean; r^2 = 0.52, n = 23, P < 0.001, for *AI* vs. standard deviation for the interspecific data set and r^2 = 0.68, n = 8, P =

0.007 for *AI* vs. mean; $r^2 = 0.95$, n = 8, $P < 0.001$, for *AI* vs. standard deviation for the data from Hall and Walter (2011)).

The use of the mean of the $\log_2$-transformed data permitted us to discriminate reliably species by pollination vector (i.e. with no errors) (Fig. 4.3a); a mean value of ~ 0.95 separated zoophilous from anemophilous species in both data sets. Similarly, an *AI* value of ~0.4 discriminated between the two pollination vectors with one error (*Plantago major*). Conversely, the standard deviation of the $\log_2$-transformed data was less effective in discriminating between vectors; a separation at ~0.85 resulted in misclassification of three anemophilous species (Figure 4.3b). On average, the mean (based on 30 flowers), standard deviation and *AI* for the ambophilous *P. lanceolata* specimens placed it among the zoophilous species.

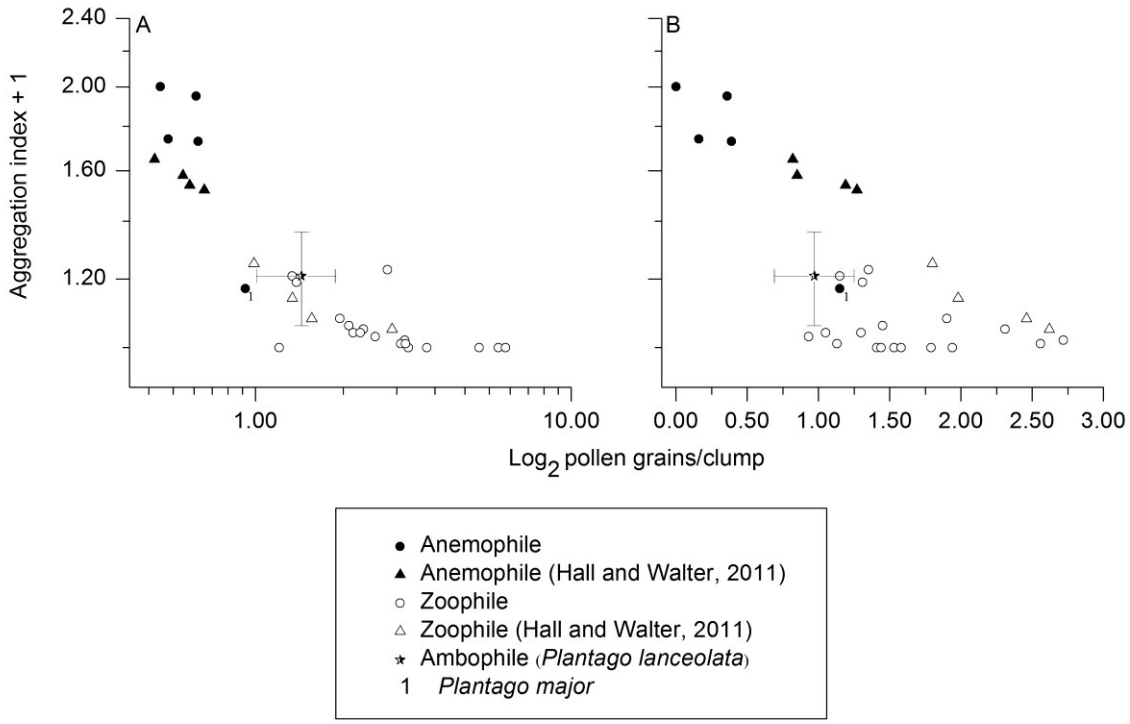

Figure 4.3: The association between the aggregation index (*AI*; a minimum estimate of proportion solitary grains; presented as *AI* + 1) and (A) the mean of the $\log_2$ (grains per clump) and (B) the standard deviation of the $\log_2$ (grains per clump) for the species presented in Table 1. Error bars represent the standard deviation.

Discussion

The lognormal distribution provided a good description of the distribution of pollen clump sizes in both anemophilous and zoophilous species. It was less effective for the distributions of pollen clump sizes in *Plantago lanceolata*, which as an ambophilous species can be expected to exhibit a combination of traits of both of the pollen vectors (e.g., the non-conforming samples had a high proportion of singletons). The distribution of pollen clumps within a species was almost always strongly right skewed, indicative of a multiplicative sequence of disaggregation events, and there were sufficient differences among the species that a measure such as the mean $\log_2$ of the pollen clump size could reliably differentiate pollen vectors. Specifically, anemophilous species appeared to have a much higher proportion of singletons than did the zoophilous species and this feature was also evident in *P. lanceolata* regardless of whether or not it fit a lognormal distribution.

As with the saltation of clumps of sand-grains on riverbeds (Visher, 1969), pollen disaggregation is expected to generate a right skewed distribution of clump sizes that becomes lognormal provided that the process was random with respect to pollen clump size and did not continue for so long that singletons (the limit) became common. In our intraspecific example of *P. lanceolata*, that 43% of the specimens did not fit a lognormal distribution indicates that there must have been large differences in the pollen clump size distributions *within the anthers* prior to release. One possible mechanism for this difference is that perhaps some anthers dehisced earlier and had had more time for disaggregation to be initiated by drying within the anther. Conversely, perhaps there is simply large variation in the amount of pollenkitt among *Plantago* anthers, due to either

genetic or developmental differences. Unhappily, it is not clear how one might measure pre-dehiscence differences in the clump size distribution without causing some disaggregation.

The interspecific distributions of pollen clump sizes were also right-skewed but as with *P. lanceolata*, some samples did not fit a lognormal distribution. The non-conforming specimens did not appear to share any obvious characteristics such as morphology or particular pollinator type (i.e., anemophily, ornithophily, entomophily and phalaenophily). As with the intraspecific comparison, there are a number of possibilities why some specimens did not fit a lognormal distribution. First, pollen within the anthers may have disaggregated to a lesser or greater degree prior to the experiment due to small differences in time since dehiscence. Alternatively, the standardized procedure for initiating disaggregation may have been too aggressive or too weak relative to the mechanisms governing granular adhesion, resulting in too much or too little disaggregation. Nonetheless, that 73-75% of species tested adhered to a lognormal distribution indicates that the method was generally effective at causing a sufficient amount of disaggregation for interspecific comparison.

Our results demonstrate that the statistical information contained within the distribution of pollen clump sizes discriminates generally between pollination vectors because there was a lower proportion of singletons among zoophiles. Even with the inclusion of samples that did not fit the lognormal distribution, measures (mean, standard deviation and *AI*) were well-correlated with one another, and found to discriminate between anemophilous and zoophilous pollination vectors, with the mean of the $\log_2$-transformed data a bit better than the other two.

There were, however, some miscategorizations. Despite its anemophilous pollination syndrome, on average, the ambophilous (based on field experiments) *P. lanceolata* fits, just barely (given the uncertainty in our metrics) (see error bars on figure 3), among zoophilous species. *P. major* also occupies this intermediate vector-space, despite its anemophilous pollination syndrome, with its mean clump size predicting anemophily and its standard deviation and *AI* predicting zoophily. Interestingly, there are accounts of ambophily in *P. major* (Kevan et al., 1993). There were also two misclassifications for anemophilous species (*Pinus tecunumanii* and *Casuarina cunninghamiana*) on the basis of their standard deviations. This suggests that standard deviation is a less reliable metric than the mean and *AI*.

It is important to realize that the vector designations given to most of the species in this study are based on pollination syndromes and anecdotal field accounts of their pollination systems. Ultimately, the utility of metrics for diagnosing pollination vectors should be substantiated using ecological studies, especially if there are intermediate ranges where multiple vectors are used by the plant. It would also be valuable to expand this data set, particularly focusing on these intermediate ranges, of which ambophily is presumed to occupy, in order to ascertain if there is a continuum in the amount of pollen clumping across pollination vectors. It could then be reasoned that there has been selection on the amount of pollen clumping in order to satisfy the physical and ecological requirements of pollen transport.

What experimental method is best suited for interspecific comparisons? Although our measures performed well with the inclusion of non-lognormal samples, as we argued above the choice of sampling methodology may result in different results; e.g., using

vibration in our intraspecific study resulted in many more non-lognormal samples than by applying an impulse as in our interspecific samples. A future study should examine a single laboratory method and ascertain how changes in impulse magnitude, relative humidity, time since the onset of dehiscence, and fall distance contribute to the development of a lognormal distribution. Further, the analysis of pollen clumping should be made using a variety of species whose pollen adhesion mechanisms differ. Following this more thorough analysis, one could then conclude the distribution of pollen clump size is a useful, simple, and reliable quantitative descriptor of pollination mode (including ambophily).

Chapter 5

General Discussion

Some well-defined patterns of floral diversity related to pollination include: (1) the convergence of floral traits among anemophilous species (i.e., independent of phylogenetic relatedness); and (2) the divergence of floral traits among closely related anemophilous and zoophilous species. These patterns are due, in part, to the contrasting biophysical requirements of anemophilous and zoophilous pollination. For example, zoophilous species must have traits that resist the release of pollen by airflows since these grains would be unavailable for collection by biotic pollinators. In contrast, anemophilous species must have traits that cause pollen to be liberated from anthers and delivered to airflows for pollination. In order to determine the evolutionary innovations of plants that differ in pollination vector, it is important understand the mechanics of wind-flower interactions. One explanation for the release of pollen among anemophilous plants is that wind causes stamens to vibrate with enough acceleration to release pollen from the anthers (Urzay et al., 2009). In this thesis I investigated whether this is a viable release mechanism in an anemophilous species, *Plantago lanceolata* (Plantaginaceae). I also measured physical parameters of stamens which could be used to quantify the relationship between floral traits and pollination vectors using a variety of species. This work is the first, to my knowledge, to empirically consider if abiotic forces in pollination apply selective pressures to flowers.

I found that during mild conditions (wind velocity < 1 m/s), *Plantago lanceolata* stamens vibrate at their natural frequency, a condition called resonance, resulting in large

amplitude vibrations that release pollen (Chapter 3). Using controlled vibrations at different frequencies in the laboratory, I found that resonance vibrations efficiently released pollen in compared to other vibration treatments. Importantly, vibration at the natural frequency minimized the energy input for release and maximized the number of pollen grains released.

According to the mechanical theory of a vibrating cantilevered beam, 3 parameters characterize the vibration response of stamens: (1) the natural frequency; (2) the damping ratio; and (3) the flexural rigidity. The natural frequency determines if the stamen interacts with kinetic-energy containing eddies (eddies whose frequencies are above the energy containing range cannot perform mechanical work), whereas the damping ratio and flexural rigidity determine the acceleration of the anther at resonance (Rao and Gupta, 1999). The measured values of each parameter corresponded with the theoretically predicted range in the analysis of wind-induced stamen vibration, further supporting the existence of this mechanism. One way in which zoophilous species may restrict wind-induced pollen release is by limiting the vibration release of pollen. By sufficiently increasing 1 or more of these parameters, it may be possible to eliminate or attenuate the vibration response. A comparison of these parameters in *P. lanceolata* with published values for a few zoophilous species suggests that this hypothesis is correct. However, a greatly expanded dataset including more anemophilous and zoophilous species, measured using the simple procedure introduced in this thesis, is needed to properly evaluate whether or not plants that differ in pollination vector also vary in their vibration response to wind gusts.

Pollen release by vibration or any other "wind-induced" mechanism (see Chapter 2) may also be facilitated or restricted via adhesion of pollen to the anther. Zoophilous plants are thought to have greater pollen adhesion than anemophilous plants owing to the production of viscin threads and tapetal fluid (see Chapter 2). To test whether or not zoophilous species have more pollen adhesion than anemophilous species, I applied standardized forces to pollen of species differing in pollination vector, which I inferred from morphological patterns, and measured the distribution of pollen clump sizes (Chapter 4). I considered pollen clumping as a proxy for adhesion strength because adhesion not only binds pollen to the anther but to other pollen grains. I found that zoophilous pollen clumps, on average, had a greater resistance to the experimentally applied disaggregating forces than anemophilous pollen clumps, suggesting that there is more pollen adhesion among zoophilous species. *Plantago lanceolata* was also included in this analysis. Interestingly, its pollen clumping placed it among zoophilous species, which was unexpected since it is primarily wind pollinated. Stelleman (1983) also found a high amount of pollen clumping in this species and hypothesized that its relatively strong pollen adhesion limits the rate of pollen release by wind permitting a minor contribution of syrphid flies to its pollination. This form of pollination, termed ambophily (pollination by wind and insects), is considered a reproductive assurance against the inherent uncertainty of wind pollination (which is essentially a random process) (Friedman, 2011).

The results of my thesis suggest that terrestrial angiosperms species may have evolved to occupy a multi-dimensional floral-trait space whose axes include physical parameters of stamens including the natural frequency, damping ratio, flexural rigidity

and pollen adhesion. However, delimiting the boundaries of each vector's space requires data from many more species. If vibration pollen release proves to be common among anemophilous species, I expect that given a large enough data set, this hypothetical space will have anemophilous and zoophilous species at opposite ends with ambophilous species occupying an intermediate position. It is also possible that other factors not considered here are responsible for restricting or promoting wind-induced pollen release. If this proves true, it might be possible to extend this scheme to include more axes representing other quantitative floral traits. For example, this hypothetical space may be extended to include regions where mechanisms other than vibration pollen release operate.

Considering pollination systems as a collection of quantitative physical parameters is novel, and in my opinion will come to replace or at least complement the traditional use of pollination syndromes for inferring the evolutionary transitions of angiosperm flowers. For example, it is thought that reduction or elimination of the perianths is a fundamental modification of angiosperms for wind pollination. However, the occurrence of ambophily in species having large petals relative to the size of the reproductive organs complicates this speculative picture. By considering flowers as combinations of physical parameters that essentially 'turn on' or 'turn off' the physical processes of anemophily (such as pollen release), it will be possible to discuss the specific innovations of a particular species for wind pollination. This will greatly improve our understanding of the evolution of flowers in response to the abiotic environment.

References

Ackerman, J.D. (2000) Abiotic pollen and pollination: ecological, functional, and evolutionary perspectives. *Plant Systematics and Evolution*, **222**, 167–185.

Ackerman, J.D. & Kevan, P.G. (2005) Abiotic Pollination. *Practical Pollination Biology* pp. 435–480. Enviroquest, Cambridge, ON, Canada.

Anonymous. (2013). Algorithm (FFT1) URL http://www.originlab.com/www/helponline/origin/en/UserGuide/Algorithm(FFT1).html [accessed 02 April 2013].

Ali, S.I. (1988) The functional significance of pollen aggregates in angiosperms. *Pakistan Journal of Botany*, **20**, 21–44.

Aylor, D.E. (1975) Force required to detach conidia of *Helminthosporium maydis*. *Plant Physiology*, **55**, 99–101.

Aylor, D.E. (2003) Rate of dehydration of corn (*Zea mays* L.) pollen in the air. *Journal of Experimental Botany*, **54**, 2307–2312.

Aylor, D.E. & Parlange, J.-Y. (1975) Ventilation required to entrain small particles from leaves. *Plant Physiology*, **56**, 97–99.

Barbosa-Cánovas, G.V., Ortega-Rivas, E., Juliano, P. & Yan, H. (2005) *Food Powders*. Springer, New York, NY, USA.

Bianchini, M. & Pacini, E. (1996) Explosive anther dehiscence in *Ricinus communis* L. involves cell wall modifications and relative humidity. *International Journal of Plant Science*, **157**, 739–745.

Blevins, R.D. (2009) Vibration of structures induced by fluid flow. *Shock and Vibration Handbook*, 6th ed (eds C. Harris, A. Piersol & T. Paez), pp. 30.1–30.67. McGraw-Hill, New York, NY, USA.

Bowker, G.E. & Crenshaw, H.C. (2007) Electrostatic forces in wind-pollination—part 1: measurement of the electrostatic charge on pollen. *Atmospheric Environment*, **41**, 1587–1595.

Buchmann, S.L. & Hurley, J.P. (1978) A biophysical model for buzz pollination in angiosperms. *Journal of Theoretical Biology*, **72**, 639–657.

Cavers, P.B., Bassett, I.J. & Crompton, C.W. (1980) The biology of Canadian weeds: 47. *Plantago lanceolata* L. *Canadian Journal of Plant Science*, **60**, 1269–1282.

Clayton, J. (2013) Optimize humidity for efficient powder handling. URL http://www.chemicalprocessing.com/articles/2013/optimize-humidity-for-efficient-powder-handling [accessed 25 May 2013]

Cruden, R.W. (1977) Pollen-ovule ratios: a conservative indicator of breeding systems in flowering plants. *Evolution*, **31**, 32–46.

Cruden, R.W. (2000) Pollen grains: why so many? *Plant Systematics and Evolution*, **222**, 143–165.

Culley, T.M., Weller, S.G. & Sakai, A.K. (2002) The evolution of wind pollination in angiosperms. *Trends in Ecology & Evolution*, **17**, 361–369.

D'Arcy, W.G. (1996) Anthers and stamens and what they do. *The Anther: Form, Function and Phylogeny* (eds W.G. D'Arcy & R.C. Keating), pp. 1–24. Cambidge University Press, Cambridge, UK.

Dahl, A., Galán, C., Hajkova, L., Pauling, A., Sikoparija, B., Smith, M. & Vokou, D. (2013) The onset, course and intensity of the pollen season. *Allergenic Pollen* (eds M. Sofiev & K.-C. Bergmann), pp. 29–70. Springer Netherlands.

Denny, M. (1988) *Biology and Mechanics of the Wave-swept Environment*. Princeton University Press, Princeton, New Jersey, USA.

Di-Giovanni, F., Kevan, P.G. & Nasr, M.E. (1995) The variability in settling velocities of some pollen and spores. *Grana*, **34**, 39–44.

Di-Giovanni, F., Kevan, P.G. & Nasr, M.E. (1996) Estimating the timing of maximum pollen release from jack pine (*Pinus banksiana* Lamb.) in northern Ontario. *The Forestry Chronicle*, **72**, 166–169.

Edlund, A.F., Swanson, R. & Preuss, D. (2004) Pollen and stigma structure and function: the Role of diversity in pollination. *The Plant Cell*, **16**, S84–S97.

Endress, P.K. (1996) Diversity and evolutionary trends in angiosperm anthers. *The Anther: Form, Function and Phylogeny* (eds W.G. D'Arcy & R.C. Keating), pp. 92–110. Cambidge University Press, Cambridge, UK.

Faegri, K. & Pijl, L. (1979) *The Principles of Pollination Ecology*. Pergamon Press, New York, NY, USA.

Fenster, C.B., Armbruster, S.W., Wilson, P., Dudash, M.R. & Thomson, J.D. (2004) Pollination syndromes and floral specialization. *Annual Review of Ecology, Evolution, and Systematics*, **35**, 375–403.

Flesch, T.K. & Grant, R.H. (1992) Corn motion in the wind during senescence: I. motion characteristics. *Agronomy Journal*, **84**, 742–747.

Franchi, G.G., Nepi, M., Dafni, A. & Pacini, E. (2002) Partially hydrated pollen: taxonomic distribution, ecological and evolutionary significance. *Plant Systematics and Evolution*, **234**, 211–227.

Franchi, G.G., Nepi, M., Matthews, M.L. & Pacini, E. (2007) Anther opening, pollen biology and stigma receptivity in the long blooming species, *Parietaria judaica* L. (Urticaceae). *Flora - Morphology, Distribution, Functional Ecology of Plants*, **202**, 118–127.

Friedman, J. (2011) Gone with the wind: understanding evolutionary transitions between wind and animal pollination in the angiosperms. *New Phytologist*, **191**, 911–913.

Friedman, J. & Barrett, S.C.H. (2009) Wind of change: new insights on the ecology and evolution of pollination and mating in wind-pollinated plants. *Annals of Botany*, **103**, 1515–1527.

Friedman, J. & Harder, L.D. (2004) Inflorescence architecture and wind pollination in six grass species. *Functional Ecology*, **18**, 851–860.

Grace, J. (1977) *Plant Response to Wind*. Academic Press, London, UK.

Grace, J. & Collins, M.A. (1976) Spore liberation from leaves by wind. *Microbiology of Aerial Plant Surfaces* (eds C.H. Dickinson & T.F. Preece), pp. 185–198. Academic Press, London, UK.

Hall, J.A. & Walter, G.H. (2011) Does pollen aerodynamics correlate with pollination vector? Pollen settling velocity as a test for wind versus insect pollination among cycads (Gymnospermae: Cycadaceae: Zamiaceae). *Biological Journal of the Linnean Society*, **104**, 75–92.

Harder, L.D. & Barclay, R.M.R. (1994) The functional significance of poricidal anthers and buzz pollination: controlled pollen removal from *Dodecatheon*. *Functional Ecology*, **8**, 509–517.

Harder, L.D. & Johnson, S.D. (2008) Function and evolution of aggregated pollen in angiosperms. *International Journal of Plant Sciences*, **169**, 59–78.

Harder, L.D. & Prusinkiewicz, P. (2012) The interplay between inflorescence development and function as the crucible of architectural diversity. *Annals of Botany*, **111**.

Henderson, L.B. (1926) Floral anatomy of several species of *Plantago*. *American Journal of Botany*, **13**, 397–405.

Hufford, L.D. & Endress, P.K. (1989) The diversity of anther structures and dehiscence patterns among Hamamelididae. *Botanical Journal of the Linnean Society*, **99**, 301–346.

Huysmans, S., El-Ghazaly, G. & Smets, E. (1998) Orbicules in angiosperms: morphology, function, distribution, and relation with tapetum types. *Botanical Review*, **64**, 240–272.

Hyde, H.A. & Williams, D.A. (1946) Studies in Atmospheric Pollen III: pollen production and pollen incidence in ribwort plantain (*Plantago lanceolata* L.). *New Phytologist*, **45**, 271–277.

Jackson, S.T. & Lyford, M.E. (1999) Pollen dispersal models in Quaternary plant ecology: assumptions, parameters, and prescriptions. *The Botanical Review*, **65**, 39–75.

Johnson, S.D. & Steiner, K.E. (2000) Generalization versus specialization in plant pollination systems. *Trends in Ecology & Evolution*, **15**, 140–143.

Jones, A.M. & Harrison, R.M. (2004) The effects of meteorological factors on atmospheric bioaerosol concentrations—a review. *Science of The Total Environment*, **326**, 151–180.

Katifori, E., Alben, S., Cerda, E., Nelson, D.R. & Dumais, J. (2010a) Foldable structures and the natural design of pollen grains. *Proceedings of the National Academy of Sciences*, **107**, 7635–7639.

Keijzer, C.J. (1987) The processes of anther dehiscence and pollen dispersal I. The opening mechanism of longitudinally dehiscing anthers. *New Phytologist*, **105**, 487–498.

Keijzer, C.J., Klooster, H.B.L. & Reinders, M.C. (1996) The mechanics of the grass flower: anther dehiscence and pollen shedding in *Maize*. *Annals of Botany*, **78**, 15–21.

Kevan, P.G., Tikhmenev, E.A. & Usui, M. (1993) Insects and plants in the pollination ecology of the boreal zone. *Ecological Research*, **8**, 247–267.

King, J.R. (1981) *Probability Charts for Decision Making*. Industrial Press, New York, NY, USA.

King, M.J. & Buchmann, S.L. (1995) Bumble bee-initiated vibration release mechanism of *Rhododendron* pollen. *American Journal of Botany*, **82**, 1407–1411.

King, M.J. & Buchmann, S.L. (1996) Sonication dispensing of pollen from *Solanum laciniatum* flowers. *Functional Ecology*, **10**, 449–456.

King, M.J. & Ferguson, A.M. (1994) Vibratory collection of *Actinidia deliciosa* (Kiwifruit) Pollen. *Annals of Botany*, **74**, 479–482.

King, M.J. & Lengoc, L. (1993) Vibratory pollen collection dynamics. *Transactions of the ASAE*, **36**, 135–140.

Kuparinen, A. (2006) Mechanistic models for wind dispersal. *Trends in Plant Science*, **11**, 296–301.

Lacey, E.P. (1996) Parental effects in *Plantago lanceolata* L. I.: a growth chamber experiment to examine pre- and postzygotic temperature effects. *Evolution*, **50**, 865–878.

de Langre, E. (2008) Effects of wind on plants. *Annual Review of Fluid Mechanics*, **40**, 141–168.

Linskens, H.F. & Cresti, M. (2000) Pollen-allergy as an ecological phenomenon: a review. *Plant Biosystems*, **134**, 341–352.

Martin, M.D., Chamecki, M. & Brush, G.S. (2010) Anthesis synchronization and floral morphology determine diurnal patterns of ragweed pollen dispersal. *Agricultural and Forest Meteorology*, **150**, 1307–1317.

Martin, M.D., Chamecki, M., Brush, G.S., Meneveau, C. & Parlange, M.B. (2009) Pollen clumping and wind dispersal in an invasive angiosperm. *American Journal of Botany*, **96**, 1703–1711.

McCartney, H.A. & Lacey, M.E. (1991) Wind dispersal of pollen from crops of oilseed rape (*Brassica napus* L.). *Journal of Aerosol Science*, **22**, 467–477.

Meléndez-Ramírez, V., Parra-Tabla, V., Kevan, P.G., Ramírez-Morillo, I., Harries, H., Fernández-Barrera, M. & Zizumbo-Villareal, D. (2004) Mixed mating strategies and pollination by insects and wind in coconut palm (*Cocos nucifera* L.

(Arecaceae)): importance in production and selection. *Agricultural and Forest Entomology*, **6**, 155–163.

Michalski, S.G. & Durka, W. (2009) Pollination mode and life form strongly affect the relation between mating system and pollen to ovule ratios. *New Phytologist*, **183**, 470–479.

Miguel, A.G., Taylor, P.E., House, J., Glovsky, M.M. & Flagan, R.C. (2006) Meteorological influences on respirable fragment release from Chinese elm pollen. *Aerosol Science and Technology*, **40**, 690–696.

Nelson, M.R., Band, L.R., Dyson, R.J., Lessinnes, T., Wells, D.M., Yang, C., Everitt, N.M., Jensen, O.E. & Wilson, Z.A. (2012) A biomechanical model of anther opening reveals the roles of dehydration and secondary thickening. *New Phytologist*, **196**, 1030–1037.

van der Niet, T. & Johnson, S.D. (2012) Phylogenetic evidence for pollinator-driven diversification of angiosperms. *Trends in Ecology & Evolution*, **27**, 353–361.

Niklas, K.J. (1985) The aerodynamics of wind pollination. *The Botanical Review*, **51**, 328–386.

Niklas, K.J. (1992) *Plant Biomechanics: An Engineering Approach to Plant Form and Function*. University of Chicago Press, Chicago, IL, USA.

Niklas, K.J. (1997) *The Evolutionary Biology of Plants*. University of Chicago Press, Chicago, IL, USA.

Olesen, J.M., Bascompte, J., Elberling, H. & Jordano, P. (2008) Temporal dynamics in a pollination network. *Ecology*, **89**, 1573–1582.

Ollerton, J. (1996) Reconciling ecological processes withphylogenetic patterns: the apparent paradox of plant-pollinator systems. *Journal of Ecology*, **84**, 767–769.

Ollerton, J., Alarcón, R., Waser, N.M., Price, M.V., Watts, S., Cranmer, L., Hingston, A., Peter, C.I. & Rotenberry, J. (2009) A global test of the pollination syndrome hypothesis. *Annals of Botany*, **103**, 1471–1480.

Pacini, E. (2000) From anther and pollen ripening to pollen presentation. *Plant Systematics and Evolution*, **222**, 19–43.

Pacini, E. & Franchi, G.G. (1996) Some cytological, ecological and evolutionary aspects of pollination. *Acta Soscietatis Botanicorum Poloniae*, **65**, 11–16.

Pacini, E. & Hesse, M. (2004) Cytophysiology of pollen presentation and dispersal. *Flora*, **199**, 273–285.

Pacini, E. & Hesse, M. (2005) Pollenkitt-its composition, forms and function. *Flora - Morphology, Distribution, Functional Ecology of Plants*, **200**, 399–415.

Pozner, R. & Cocucci, A. (2006) Floral structure, anther development, and pollen dispersal of *Halophytum ameghinoi* (Halophytaceae). *International Journal of Plant Sciences*, **167**, 1091–1098.

Primack, R.B. (1978) Evolutionary aspects of wind pollination in the genus *Plantago* (Plantaginaceae). *New Phytologist*, **81**, 449–458.

Proctor, M., Yeo, P. & Lack, A. (1996) *The Natural History of Pollination*. Harper Collins Publishers, London, UK.

Rao, J.S. & Gupta, D.K. (1999) *Introductory Course on Theory and Practice of Mechanical Vibrations*. New Age International. New Delhi, India.

Rhodes, M. (2008) *Introduction to Particle Technology*. John Wiley & Sons. Hoboken, NJ, USA.

Sabban, L., Jacobson, N.-L. & van Hout, R. (2012) Measurement of pollen clump release and breakup in the vicinity of ragweed (*A. confertiflora*) staminate flowers. *Ecosphere*, **3**, 1–24.

Sahli, H.F. & Conner, J.K. (2006) Characterizing ecological generalization in plant-pollination systems. *Oecologia*, **148**, 365–372.

Schlitching, H. & Gersten, K. (2000) *Boundary Layer Theory.* Springer, Berlin.

Sharma, N., Koul, A.K. & Kaul, V. (1999) Pattern of resource allocation of six *Plantago* species with different breeding systems. *Journal of Plant Research*, **112**, 1–5.

Stelleman, P. (1984a) The significance of biotic pollination in a nominally anemophilous plant: *Plantago lanceolata*. *Proceedings of the Koninklijke Nederlandse Akademie van Wetenschappen*, **87**, 95–119.

Stelleman, P. (1984b) Reflections on the transition from wind pollination to ambophily. *Acta Botanica Neerlandica*, **33**, 497–508.

Sterling, M., Baker, C.., Berry, P.. & Wade, A. (2003) An experimental investigation of the lodging of wheat. *Agricultural and Forest Meteorology*, **119**, 149–165.

Taylor, P.E., Card, G., House, J., Dickinson, M.H. & Flagan, R.C. (2006) High-speed pollen release in the white mulberry tree, Morus alba L. *Sexual Plant Reproduction*, **19**, 19–24.

Taylor, P.E., Flagan, R.C., Miguel, A.G., Valenta, R. & Glovsky, M.M. (2004) Birch pollen rupture and the release of aerosols of respirable allergens. *Clinical & Experimental Allergy*, **34**, 1591–1596.

Taylor, P.E., Flagan, R.C., Valenta, R. & Glovsky, M.M. (2002) Release of allergens as respirable aerosols: a link between grass pollen and asthma. *Journal of Allergy and Clinical Immunology*, **109**, 51–56.

Tonsor, S.J. (1985) Intrapopulational variation in pollen-mediated gene flow in *Plantago lanceolata* L. *Evolution*, **39**, 775–782.

Urzay, J., Llewellyn Smith, S.G., Thompson, E. & Glover, B.J. (2009) Wind gusts and plant aeroelasticity effects on the aerodynamics of pollen shedding: A hypothetical

turbulence-initiated wind-pollination mechanism. *Journal of Theoretical Biology*, **259**, 785–792.

Visher, G.S. (1969) Grain size distributions and depositional processes. *Journal of Sedimentary Research*, **39**, 1079–1106.

Vroege, P.W. & Stelleman, P. (1990) Insect and wind pollination in *Salix repens* L. and Salix caprea L. *Israel Journal of Botany*, **39**, 125–132.

Walton, O.R. (2008) Review of adhesion fundamentals for micro-scale particles. *KONA Powder and Particle Journal*, 129–141.

Waser, N.M., Chittka, L., Price, M.V., Williams, N.M. & Ollerton, J. (1996) Generalization in pollination systems, and why it matters. *Ecology*, **77**, 1043–1060.

Whitaker, D.L., Webster, L.A. & Edwards, J. (2007) The biomechanics of *Cornus canadensis* stamens are ideal for catapulting pollen vertically. *Functional Ecology*, **21**, 219–225.

Wyngaard, J.C. (2010) *Turbulence in the Atmosphere*. Cambridge University Press. Cambridge, UK.

Young, K.A. & Schmitt, J. (1995) Genetic variation and phenotypic plasticity of pollen release and capture height in *Plantago lanceolata*. *Functional Ecology*, **9**, 725–733.